Monthly Notices
of the
ROYAL ASTRONOMICAL SOCIETY

Mon. Not. R. Astron. Soc. **402,** 2369–2387 (2010) doi:10.1111/j.1365-2966.2009.16093.x

Identifying birth places of young isolated neutron stars

N. Tetzlaff,[1⋆] R. Neuhäuser,[1] M. M. Hohle[1,2] and G. Maciejewski[1]

[1]*Astrophysikalisches Institut und Universitäts-Sternwarte Jena, Schillergässchen 2-3, 07745 Jena, Germany*
[2]*Max-Planck-Institut für extraterrestrische Physik, Giessenbachstraße, 85741 Garching, Germany*

Accepted 2009 November 23. Received 2009 November 4; in original form 2009 September 15

ABSTRACT

Young isolated radio-quiet neutron stars are still hot enough to be detectable at X-ray and optical wavelengths due to their thermal emission and can hence probe cooling curves. An identification of their birth sites can constrain their age.

For that reason, we try to identify the parent associations for four of the so-called Magnificent Seven neutron stars for which proper motion and distance estimates are available. We are tracing back in time each neutron star and possible birth association centre to find close encounters. The associated time of the encounter expresses the kinematic age of the neutron star which can be compared to its characteristic spin-down age. Owing to observational uncertainties in the input data, we use Monte Carlo simulations and evaluate the outcome of our calculations statistically.

RX J1856.5−3754 most probably originated from the Upper Scorpius association about 0.3 Myr ago. RX J0720.4−3125 was either born in the young local association TW Hydrae about 0.4 Myr ago or in Trumpler 10 0.5 Myr in the past. Also RX J1605.3 + 3249 and RBS 1223 seem to come from a nearby young association such as the Scorpius-Centraurus complex or the extended Corona-Australis association. For RBS 1223 also a birth in Scutum OB2 is possible.

We also give constraints on the observables as well as on the radial velocity of the neutron star. Given the birth association, its age and the flight time of the neutron star, we estimate the mass of the progenitor star.

Some of the potential supernovae were located very nearby (<100 pc) and thus should have contributed to the ^{10}Be and ^{60}Fe material found in the Earth's crust.

In addition, we reinvestigate the previously suggested neutron star/runaway pair PSR B1929+10/ζ Ophiuchi and conclude that it is very likely that both objects were ejected during the same supernova event.

Key words: stars: kinematics – pulsars: individual: PSR B1929 + 10 – pulsars: individual: RX J1856.5−3754 – pulsars: individual: RX J0720.4−3125 – pulsars: individual: RX J1605.3 + 3249 – pulsars: individual: RBS 1223.

1 INTRODUCTION

Neutron stars have very large proper motions which, with known distances, indicate high space velocities (e.g. Lyne & Lorimer 1994; Hansen & Phinney 1997; Lorimer, Bailes & Harrison 1997; Cordes & Chernoff 1998; Arzoumanian, Chernoff & Cordes 2002; Hobbs et al. 2005, thereafter Ho05). Those high velocities that are usually larger than those of the progenitor stars are the result of asymmetric supernova (SN) explosions assigning the new-born neutron star a kick velocity for that a number of mechanisms have been suggested (e.g. Burrows & Hayes 1996; Janka & Mueller 1996; Janka et al. 2005; Wang, Lai & Han 2006; Kisslinger, Henley & Johnson 2009).

Another fact is that about 46 per cent of O and 10 per cent of B stars also show high space velocities (see Stone 1991 for a discussion). Two scenarios (Hoogerwerf, de Bruijne & de Zeeuw 2001, thereafter H01) are accepted to produce those so-called 'runaway stars' (Blaauw 1961). The binary- SN scenario is related to the formation of the high-velocity neutron stars: the runaway and neutron star are the products of a SN within a binary system. The velocity of the former secondary is comparable to its original orbital velocity. The second scenario, which will not be further discussed within this paper, is the dynamical ejection due to gravitational interactions between massive stars in dense clusters. H01 proposed examples for each of the scenarios. In Section 4, we will review and further investigate the binary SN scenario for PSR B1929+10 and the runaway O9.5V star ζ Oph. Instead of restricting the unknown pulsar radial

⋆E-mail: nina@astro.uni-jena.de

velocity to a certain interval, we will use a velocity distribution to cover the whole spectrum of possible radial velocities. We then use more recent data for the pulsar to strengthen the hypothesis.

Beforehand, we introduce our sample of OB associations and clusters in Section 2 and the procedure utilized in Section 3.

In Section 5, we investigate the origin of four isolated radio-quiet X-ray emitting neutron stars. So far, seven such sources have been confirmed. They are not only bright X-ray sources, but also detected in the optical due to a hot cooling surface. In two cases, a parallax is obtained. Brightness, parallax and temperature yield their radii. From spectra, one can in principle determine their mass and composition, which eventually may lead to constraints on the equation of state. However, only seven such sources have been identified up to now for which they were named 'The Magnificent Seven' (M7) (Treves et al. 2001; for a recent review see Kaplan 2008; two new candidates were recently published by Pires et al. 2009; Rutledge, Fox & Shevchuk 2008). With known luminosity, one only needs to estimate the age, in order to probe cooling curves. For young neutron stars, the characteristic spin-down age only gives an upper limit. We will therefore try to estimate their age from kinematics.

Our aim in this paper is to identify the parent associations of four members of the M7 and find constraints on their observables and radial velocity.

We give a summary of our results and draw our conclusions in Section 6.

2 THE SAMPLE OF ASSOCIATIONS AND CLUSTERS

Given a distance of 1 kpc and typical neutron star velocities of 100–500 km s^{-1} (Arzoumanian et al. 2002; Ho05) and maximum ages of 5 Myr for neutron stars to be detectable in the optical (see cooling curves in Gusakov et al. 2005 and Popov, Grigorian & Blaschke 2006), we restricted our search for birth associations and clusters of young nearby neutron stars to within 3 kpc. We chose a sample of OB associations and young clusters (we use the term 'association' for both in the following) within 3 kpc from the Sun with available kinematic data and distance. We collected those from Dambis, Mel'nik & Rastorguev (2001) and H01 and associations to which stars from the Galactic O-star catalogue from Maíz-Apellániz et al. (2004) are associated with. Furthermore, we added young local associations (YLA) from Fernández, Figueras & Torra (2008) (thereafter F08) since they are possible hosts of a few SNe in the near past. We also included the Hercules–Lyrae association (Her–Lyr) and the Pleiades and massive star-forming regions (Reipurth 2008a,b). We set the lower limit of the association age to $\approx$2 Myr to account for the minimum lifetime of a progenitor star that can produce a neutron star (progenitor mass smaller than $\approx 30\,M_{\odot}$; see e.g. Heger et al. 2003).[1] The list of all explored associations and their properties can be found in Appendix A. Coordinates as well as heliocentric velocity components are given for a right-handed coordinate system with the x-axis pointing towards the galactic centre and y is positive in the direction of galactic rotation.

[1]The minimum lifetime is actually $\approx$6 Myr. We relax that condition to account for possible uncertainties in the association age as well as the fact that also more massive stars may produce neutron stars (Belczynski & Taam 2008).

3 PROCEDURE

To identify potential parent associations of neutron stars, we calculate the trajectories for both, the neutron star and the centre of the association, into the past. We account for solar motion adopting a local standard of rest of $(\mathrm{UVW})_{\odot} = (10.00\ 5.25\ 7.17)\,\mathrm{km\,s^{-1}}$ (Dehnen & Binney 1998). To include the effect of a potential on the vertical motion, we use the vertical acceleration from Perrot & Grenier (2003) (and references therein) and work with an Euler–Cauchy numerical method with a fixed time-step of 10^4 yr. Utilizing this simple technique is fully sufficient for the treatment of some million years as done here and is consistent with results obtained by applying a fifth-order Runge–Kutta integration method for a more complicated potential as e.g. given in Harding et al. (2001) and references therein (cf. comparison of methods in Tetzlaff 2009).

Simultaneously to the trajectories, we derived the separation between the neutron star and the association centre for each time-step, and found the minimum of those as well as the associated time in the past. Since the input consists of observables with errors, we calculate a large set of simulations varying the starting parameters normally (proper motion and parallax;[2] radial velocity see below) within their confidence levels.

For neutron stars, the radial velocity cannot easily be derived from spectra due to the large gravitational redshift and hence is unknown. To be able to investigate their 3D motion none the less, we varied the radial velocity within a probability distribution derived from the one for 3D pulsar velocities obtained by Ho05. They deducted a distribution with one Maxwellian component from transverse velocities of 233 pulsars assuming the radial component is of the same order. Arzoumanian et al. (2002) derived a distribution that includes two Maxwellian components suggesting that there might be two different populations: those which gained their speed only due to a kick during the SN and those which have an additional component from their former orbital velocity. However, as stated by Ho05, a one-component model better fits the observations. Infact, which radial velocity distribution is used is of minor importance since its usage will just assure that the whole spectra of possible radial velocities are covered and the probability of occurrence of excessively high values is low which is the case for both distributions. Adopting the two-component model does not affect the final results significantly (Tetzlaff 2009). As the sign of the radial velocity cannot be derived from statistics it was chosen randomly, thus covering a total range of -1500 to $+1500\,\mathrm{km\,s^{-1}}$.

4 A POTENTIAL BINARY SN IN UPPER SCORPIUS

The runaway O-star ζ Ophiuchi (ζ Oph = HIP 81377) is an isolated main sequence star with a space velocity of $\approx$20 km s^{-1}. Blaauw (1952) suggested its origin in the Scorpius OB2 association due to its proper motion vector which points away from that association.

H01 investigated the origin of ζ Oph in more detail and proposed that it gained its high velocity in a binary SN in Upper Scorpius (US) about 1 Myr ago which is also supported by its large rotational velocity of $\geq$340 km s^{-1} (Herrero et al. 1992; Penny 1996; Howarth & Smith 2001) and high helium abundance (Herrero et al. 1992; van Rensbergen, Vanbeveren & de Loore 1996; Villamariz & Herrero 2005). They also identified a neutron star which might have been the former primary: PSR B1929 + 10 (PSR J1932 + 1059).

[2]For some cases, we obtain the parallax from other distance estimates.

Table 1. Properties of PSR B1929 + 10 and ζ Oph (μ_α^* is the proper motion in right ascension corrected for declination). Note that the radial velocity of the pulsar is an assumption from H01, not a measurement.

	$\alpha(^\circ)$	$\delta(^\circ)$	π(mas)	μ_α^*(mas yr^{-1})	μ_δ(mas yr^{-1})	v_r(km s^{-1})	Ref.
PSR B1929+10 (H01)	293.06	10.99	4 ± 2	99 ± 12	39 ± 8	200 ± 50	1
PSR B1929+10 (recent)	293.06	10.99	2.76 ± 0.14	94.03 ± 0.14	43.37 ± 0.29	–	2
ζ Oph	249.29	−10.57	7.12 ± 0.71	13.07 ± 0.85	25.44 ± 0.72	-9.0 ± 5.5	3, 4

1 – H01 and references therein, 2 – Chatterjee et al. (2004), 3 – *Hipparcos* Catalogue, 4 – *Hipparcos* Input Catalogue.

Initially, we repeat the experiment of H01 applying the same starting parameters for the pulsar (Table 1, μ_α^* is the proper motion in right ascension corrected for declination). Note that the pulsar radial velocity of 200 ± 50 km s^{-1} is not measured, but an assumption in H01. The runaway proper motion and parallax were adopted from the *Hipparcos* Catalogue (Perryman et al. 1997) and its radial velocity from the *Hipparcos* Input Catalogue (Turon et al. 1992). The results are in very good agreement with those of H01. 29 700 of 3 million Monte Carlo runs yield a minimum separation between ζ Oph and PSR B1929 + 10 of less than 10 pc compared to 30 822 runs as published by H01. The smallest separation we found was 0.20 pc (0.35 pc found by H01). In 4631 runs, both objects were additionally not farther from the centre of US than 10 pc. The latter number differs slightly from that of H01 (4210 runs) which is owing to somewhat different input parameters for the association.

Similar calculations were also done by Bobylev (2008) with the same results using the epicycle approximation (Lindblad 1959; Wielen 1982) for tracing back the objects. Afterwards, he used more recent parameter values for the pulsar from Chatterjee et al. (2004), but increased the error intervals (a factor of 10 for the parallax, a factor of 30 for the proper motion components), to have them of the same order as H01 before, and drew the conclusion that the scenario of a binary SN in US involving the two objects is very likely.

We reinvestigate the issue as well using a radial velocity distribution (Section 3) instead of a specified interval. In 3 million Monte Carlo runs the smallest separation found was 4.0 pc. This is too large to support the hypothesis that ζ Oph and PSR B1929 + 10 once were at the same position at the same time in the past. However, the errors of the parallax and the proper motion components of the pulsar (Table 1) are very small and thus might be underestimated due to unknown systematical effects. For that reason, we as well increase them by a factor of 10. The smallest difference in position then was 0.2 pc which is consistent with the binary SN scenario. We select those minimum separations for which both, the pulsar and the runaway, were not more than 15 pc away from the centre of US. Of 3 million runs, 5367 fulfilled this requirement. The slope of the resulting histogram in Fig. 1(a) can be explained with a 3D Gaussian distribution of the separation (see H01 for details),

$$W_{3D}(\Delta) = \frac{\Delta}{2\sqrt{\pi}\sigma\mu}\left\{exp\left[-\frac{1}{2}\frac{(\Delta-\mu)^2}{2\sigma^2}\right] - exp\left[-\frac{1}{2}\frac{(\Delta+\mu)^2}{2\sigma^2}\right]\right\}, \quad (1)$$

and in the limit $\mu \to 0$

$$W_{3D,\mu\to 0}(\Delta) = \frac{\Delta^2}{2\sqrt{\pi}\sigma^3}\exp\left[-\frac{\Delta^2}{4\sigma^2}\right], \quad (2)$$

respectively, either with $\mu = 0 \pm 5.6$ pc or $\mu = 9.0 \pm 4.0$ pc. Δ denotes the 3D separation $| x_{\rm pulsar} - x_{\zeta\,\rm Oph} |$ between the pulsar and the runaway, μ and σ are the expectation value and the standard deviation, respectively, and $\pi = 3.1459\ldots$. The agreement to the curves is remarkable. Fig. 2 shows the correlation between minimum separations and corresponding times. It can be seen that there is a small spread in time for larger separations which is owing to the deviations from a Gaussian distribution and the actual 4D problem since the time is involved as well.

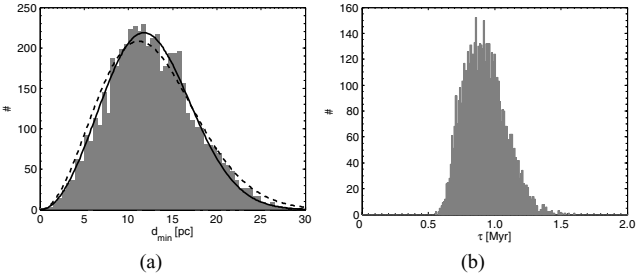

Figure 1. (a) Distribution of minimum separations $d_{\rm min}$ of the 5367 runs for which both objects were not farther than 10 pc from the US centre with updated pulsar data. Drawn as well are theoretical curves for 3D Gaussian distributions (equations 1 and 2) with $\mu = 9.0$ pc and $\sigma = 4.0$ pc (solid) and $\mu = 0$ and $\sigma = 5.6$ pc (dashed), respectively. Note that these are not fitted to the data. (b) Distribution of corresponding flight times τ in the past since the SN.

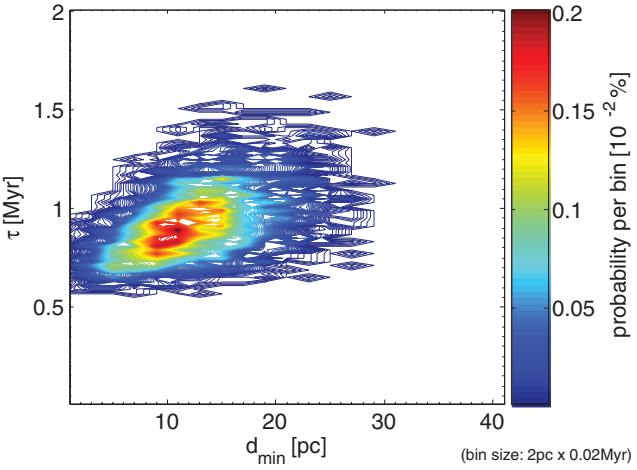

Figure 2. $\tau - d_{\rm min}$ contour plot to Fig. 1.

Adopting that PSR B1929 + 10 and ζ Oph were ejected in the same SN about 1 Myr ago in US, we find that the pulsar would now have a radial velocity of $\approx$250 km s^{-1} which is close to the value of 200 ± 50 km s^{-1} H01 adopted previously. The distance to the Sun of this SN event 1 Myr ago was 154 ± 7 pc (note that this error quotes a 68 per cent confidence interval but is not a 1σ error, though).

Given an age of 5 Myr for US (de Geus, de Zeeuw & Lub 1989; Preibisch et al. 2002), we can estimate the mass of the progenitor star of PSR B1929 + 10 assuming that star formation happened

Table 2. Parameters of four of the M7. Note that only for RX J1856.5−3754 and RX J0720.4−3125 π denotes trigonometric parallax measurements whereas for RX J1605.3 + 3249 and RBS 1223 distance limits are model estimates (from brightness and extinction compared to RX J1856.5−3754 and RX J0720.4−3125).

	$\alpha(^\circ)$	$\delta(^\circ)$	π(mas)	μ_α^* (mas yr^{-1})	μ_δ (mas yr^{-1})	$n_{\rm H}$ (10^{20} cm^{-2})	Ref.
RX J1856.5-3754	284.15	−37.91	5.6 ± 0.6	326.7 ± 0.8	-59.1 ± 0.7	0.74 ± 0.10	2, 3, 7
RX J0720.4-3125	110.10	−31,43	2.77 ± 1.29	-93.9 ± 2.2	52.8 ± 2.3	1.04 ± 0.02	8, 10
RX J1605.3+3249	231.33	32.82	>2.4	-43.7 ± 1.7	148.7 ± 2.6	1.1 ± 0.4	1, 5, 9
RBS 1223	197.20	21.45	1.4–13	-207 ± 20	84 ± 20	1.8 ± 0.2	4, 6, 9

References: 1 – Motch et al. (1999), 2 – Kaplan, van Kerkwijk & Anderson (2002), 3 – Kaplan (2003), 4 – Schwope et al. (2005), 5 – Zane et al. (2006), 6 – Schwope et al. (2007) (their model 3), V. Hambaryan (priv. comm.), 7 – Posselt et al. (2007), 8 – Kaplan et al. (2007), 9 – Motch et al. (2007), 10 – Hohle et al. (2009).

contemporaneously, i.e that the progenitor exploded (5–1) Myr after birth. Evolutionary models from Tinsley (1980) (thereafter T80), Maeder & Meynet (1989) (thereafter MM89) and Kodama (1997) (thereafter K97) (see also Romano et al. 2005 for a review) yield a progenitor mass of 44, 38 and 32 $M_\odot$, respectively, for a star with a lifetime of 4 Myr assuming solar metallicity, corresponding to a spectral type of O6 to O7 on the main sequence (Schmidt-Kaler 1982). According to Sartori, Lépine & Dias (2003) US is somewhat older, namely 8–10 Myr. This association age range would imply a smaller progenitor mass of 18 (B0V) to 37 $M_\odot$ (O6V) (depending on the evolutionary model) which is in better agreement to the upper star mass limit of $\approx$30 $M_\odot$ (Heger et al. 2003) for formation of a neutron star. However, owing to mass transfer during binary evolution also more massive stars may produce neutron stars (Belczynski & Taam 2008).

The O9.5V star ζ Oph has a mass of 20 $M_\odot$ [derived from isochrones by Schaller et al. (1992), Bertelli et al. (1994) and Claret (2004) for solar metallicity; table in Schmidt-Kaler (1982)].

If ζ Oph was ejected in a SN, the progenitor star should have an earlier spectral type, consistent with our results. With the additional constraint that the SN produced a neutron star, i.e. the progenitor was later than $\approx$O6 to O7, the progenitor star was O6/O7 to O9.

It may not be justified to enlarge the errors of the input parameters of the pulsar. With the published small error bars, we cannot confirm that ζ Oph was at the same position in space at the same time as PSR B1929+10, but may have been ejected by a different SN event in US.

5 IDENTIFYING PARENT ASSOCIATIONS AND CLUSTERS FOR YOUNG ISOLATED NEUTRON STARS

For four of the M7 distance estimates and proper motion values are available and thus their birth sites can in principle be found if assumptions on the radial velocity are made. Table 2 gives their properties.

We trace back the objects for 5 Myr. As a first step, we perform 1 00 000 runs for each neutron star and all 140 associations in the sample. Those associations for which the smallest separation found was less than three times the association radius or less than 100 pc were chosen for a more detailed investigation with 2 million runs. We give the results of the latter in the following sections.

5.1 RX J1856.5−3754

Investigating probable birth places of RX J1856.5−3754, nine of the 140 associations yield a smallest separation between the neutron star and the association centre found after another 2 million runs which was consistent with the respective association radius[3] (see Table 3). However, only five of the other associations show a peak in the $\tau - d_{\rm min}$ contour plot which also lies within the association boundaries or at least intersects. Table 4 lists the respective associations along with the results of the investigation including 2 million runs with varying input parameters. Columns 2 and 3 of that table specify a region in the $\tau - d_{\rm min}$ contour diagram with higher probability than its surroundings (see Appendix B). Columns 4–8 give values for the present-day properties which RX J1856.5−3754 would have if it originated from the particular association. The space velocity $v_{\rm space}$ which corresponds to the ejection speed of the neutron star in the SN is given in Column 7. Assuming that the ejection speed is of the same amount as the kick velocity, this value gives an upper limit of the latter.[4]

Table 3. Associations for which the smallest separation between RX J1856.5−3754 and the association centre found (min. $d_{\rm min}$) after 2 million runs was within the radius of the association. Column 2 gives the smallest separation, Column 3 the radius of the association (see Appendix A for references).

Association	min. $d_{\rm min}$ (pc)	$R_{\rm Assoc}$ (pc)
US	0.4	15
Tuc-Hor	46.1	50
β Pic-Cap	26.3	57
Ext. R CrA	4.4	31
AB Dor	32.0	45
Her-Lyr	10.4	13
Sgr OB5	64.1	111
Sco OB4	19.0	33
Pismis 24	1.6	2
Tr 27	1.8	6

The last three columns indicate the position of the potential SN at the corresponding time with the distance to the Sun and equatorial coordinates. For how those values are derived, please see Appendix B.

From Table 4, we conclude that the most likely parent association for RX J1856.5−3754 is either US, the extended Corona–Australis association (Ext. R CrA) or Scorpius OB4 (Sco OB4).

[3]Considering the present radius of an association ensures that we do not miss potential SNe that might have occurred near the edge. The former radius was surely smaller than the present one.

[4]The kick velocity strongly depends on whether the progenitor star was single or not and in the case of binarity also on the separation between the stars. However, SN kick theory predicts kick velocity distributions which are consistent with observed neutron star velocities (e.g. Scheck et al. 2006; Ng & Romani 2007; Kuranov, Popov & Postnov 2009).

Table 4. Potential parent associations of RX J1856.5−3754. Columns 2 and 3 mark the boundaries of a 68 per cent area in the $\tau - d_{\rm min}$ contour plot for which the current neutron star parameters (Columns 4–7, radial velocity $v_{\rm r}$, proper motion μ_α^* and μ_δ and parallax π) were obtained, and Columns 8–10 indicate the distance to the Sun $\rm d_\odot$ and equatorial coordinates (J2000.0) of the potential SN. Column 7 gives the space velocity (ejection speed) $v_{\rm space}$ derived from proper motion and radial velocity. For the deduction of the values given in Columns 4–11, please see Appendix B.

Association	$d_{\rm min}$ (pc)	τ (Myr)	$v_{\rm r}$ (km s^{-1})	$\mu_{\alpha*}$ (mas yr^{-1})	μ_δ (mas yr^{-1})	$v_{\rm space}$ (km s^{-1})	π (mas)	$\rm d_\odot$ (pc)	α (°)	δ (°)
US	5...3	0.28...0.34	193^{+45}_{-32}	326.7 ± 0.8	-59.1 ± 0.7	349^{+40}_{-32}	$5.41^{+0.33}_{-0.28}$	140...163	$243.21^{+0.56}_{-0.52}$	$-23.66^{+0.31}_{-0.29}$
β Pic-Cap	35...53	0.10...0.15	1190^{+167}_{-172}	326.7 ± 0.8	-59.1 ± 0.7	1222^{+165}_{-173}	$5.71^{+0.49}_{-0.24}$	40^{+5}_{-5}	221...233	−18...−8
Ext. R CrA	26...54	0.10...0.15	406^{+121}_{-88}	326.7 ± 0.8	-59.1 ± 0.7	492^{+113}_{-81}	$5.68^{+0.35}_{-0.37}$	127^{+6}_{-6}	$256.76^{+2.06}_{-2.02}$	$-33.72^{+0.63}_{-0.61}$
AB Dor	44...60	0.12...0.16	1146^{+138}_{-152}	326.7 ± 0.8	-59.1 ± 0.7	1177^{+137}_{-151}	$5.88^{+0.30}_{-0.27}$	32...46	$210.19^{+6.41}_{-4.13}$	$0.90^{+2.80}_{-5.72}$
Sco OB4	25...33	1.26...1.51	-604^{+31}_{-20}	326.7 ± 0.8	-59.1 ± 0.7	664^{+25}_{-35}	$5.72^{+0.32}_{-0.30}$	1092^{+2}_{-2}	$259.84^{+0.69}_{-0.69}$	$-31.66^{+0.85}_{-0.34}$

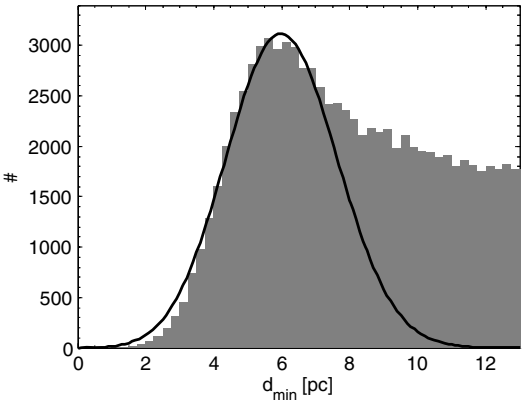

Figure 3. Distribution of minimum separations $d_{\rm min}$ between RX J1856.5−3754 and the centre of US within the defined time range τ (see Table 4, Column 3). Shown as well is a theoretical curve for a 3D Gaussian distribution (equation 1) with $\mu = 5.5$ pc and $\sigma = 1.2$ pc. Note that the curve is not a fit to the data but will just give an explanation of the slope of the histogram. The disagreement on the right-hand side of the diagram is due to the actual 4D problem since the time is involved. Furthermore, natural discrepancies to a Gaussian distribution occur since parallaxes are taken to obtain positions and a Maxwellian distribution is utilized for the velocities. Unlike in the previous section, we cannot restrict to a certain number of runs owing to a third component (in the case of PSR B1929/ζ Oph the distance to US) which gives constraints on the time.

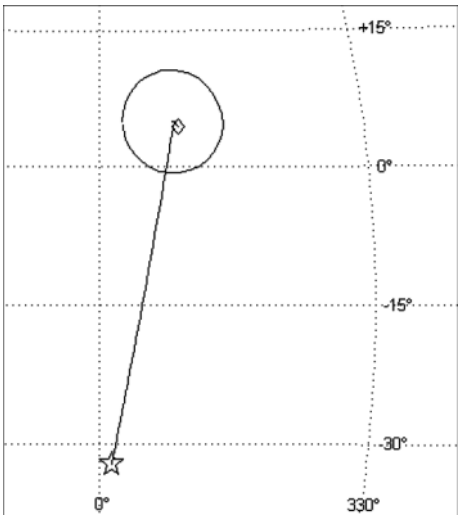

Figure 4. Past trajectories for RX J1856.5−3754 and US projected on a Galactic coordinate system (for a particular set of input parameters consistent with Table 4). Present positions are marked with a star for the neutron star and a diamond for the association. The large circle reflects an association radius of 15 pc.

For the two remaining – the β Pictoris group (β Pic-Cap) and AB Doradus (AB Dor) – the radial needed velocities would be excessively high (>1000 km s^{-1}, space velocities $v_{\rm space} > 1000$ km s^{-1}), thus making them unlikely (see Ho05) to host the birth place of RX J1856.5−3754. The probability of those two associations of being the birth associations is more than 4000 times smaller than for the other three (for deviation of the probability, please see Appendix B).

Since the smallest separation found for Sco OB4 (19 pc) is relatively high compared to those of US (<1 pc) and Ext. R CrA (< 5 pc), and the modulus of the radial velocity needed of ≈600 km s^{-1} (Column 4 of Table 4) is rather high (space velocity ≈665 km s^{-1}), Sco OB4 may be less likely the birth place of RX J1856.5−3754. For Ext. R CrA, the potential place of the SN lies between 26 and 44 pc away from the association centre. The radius of Ext. R CrA is 31 pc, thus the SN should have occurred near the edge of the association. In comparison to that, a SN in US which produced RX J1856.5−3754 would have taken place at 5.5 ± 1.2 pc from the centre of US (Fig. 3) which has a radius of 15 pc. As SNe are supposed to occur in denser regions of an association, the latter scenario thus seems most likely. Furthermore, the probability of US being the parent association of RX J1856.5−3754 is 10 times larger than that for Ext. R CrA and eight times larger than for Sco OB4.

The origin of RX J1856.5−3754 has also been previously suggested by Walter & Lattimer (2002) to lie within the US association ≈0.5 Myr ago as the projected trajectory of RX J1856.5−3754 crosses the projection of US. Here, we find a kinematic age of ≈0.3 Myr.

In this case (Fig. 4), the neutron star would now have a radial velocity of ≈190 km s^{-1}. The space velocity of ≈340 km s^{-1} in this case is close to the peak of the velocity distribution for pulsars from Ho05.

Walter et al. (2000) suggested that ζ Oph was the former secondary of RX J1856.5−3754 that exploded a few Myr ago in US. Therefore, we re-investigate the separation between RX J1856.5−3754 and the runaway star as well as their separation to the centre of US. Out of 3 million runs the smallest separation found between the neutron star and ζ Oph was 22 pc which is far too large to support this former binary hypothesis.

Given the age of US of 5 Myr (de Geus et al. 1989), we estimate the mass of the progenitor star (lifetime 4.7 Myr) to be, depending on the model, 45 $\rm M_\odot$ (T80), 41 $\rm M_\odot$ (MM89) and 35 $\rm M_\odot$ (K97) (spectral type ≈O6.5, Schmidt-Kaler 1982). Using the more recent age determination for the Sco-Cen associations by Sartori et al.

Table 5. Associations for which the smallest separation between RX J0720.4−3125 and the association centre found (min. $d_{\rm min}$) after 2 million runs was within the radius of the association, as Table 3.

Association	min. $d_{\rm min}$ (pc)	$R_{\rm Assoc}$ (pc)
US	11.8	15
UCL	27.5	33
LCC	18.2	23
TWA	0.1	33
Tuc-Hor	37.6	50
β Pic-Cap	18.2	57
HD 141569	4.7	16
Pup OB1	6.0	65
Pup OB3	0.5	15
NGC 2546	6.6	10
Tr 10	17.3	23
Cha T	0.8	21

(2003) of 8–10 Myr for US, we estimate the mass of the progenitor star of RX J1856.5−3754 to be between 17 and 35 $M_\odot$ (B0 to O7 on the main sequence). Currently, the earliest spectral type in US is B0. Hence, our assumption of contemporary star formation and our result on the progenitor spectral type are consistent with the progenitor star of RX J1856.5−3754 being earlier than the earliest present member star.

Since Walter & Lattimer (2002) published a significant different parallax for RX J1856.5−3754 of $\pi = 8.5 \pm 0.9$ mas, we repeat our simulations adopting this value. The overall picture of potential parent associations remains (cf. Table 3).[5] Still, US is the most probable association to have hosted the SN which formed RX J1856.5−3754. While the position of this SN using Walter's parallax does not significantly change, the neutron star's current parallax would be $\pi = 7.44^{+1.27}_{-0.48}$ mas and the radial velocity needed $v_{\rm r} = -25^{+58}_{-24}$ km s^{-1}. Furthermore, the kinematic age would be slightly larger, $\tau \approx 0.5$ Myr (confirming the result of Walter & Lattimer 2002), implying a progenitor mass of 37– 45 $M_\odot$ ($\approx$O6.5 on the main sequence) adopting an age of US of 5 Myr or 17– 29 $M_\odot$ (B0 to O7 on the main sequence) for an association age of 10 Myr (T80; MM89; K97).

We again investigated the RX J1856.5−3754/ ζ Oph binary scenario using the larger parallax as an input. Out of 2 million runs, we found a smallest separation of 20 pc ruling out this hypothesis.

5.2 RX J0720.4−3125

For RX J0720.4−3125, 12 associations were identified for which the smallest separation between the neutron star and the association centre found in the past after 2 million runs lied within the respective association boundaries (see Table 5). Five of those show a peak in the $\tau - d_{\rm min}$ contour plot at values of $d_{\rm min}$ that at least intersect the association. For the Chamaeleon-T association (Cha T) only a very small fraction of runs yield small distances, thus we exclude it as a probable parent association for RX J0720.4−3125. Analogues to Table 4 for RX J1856.5−3754, they are given in Table 6 along with the separation and corresponding time ranges in the past defined by the peak in the $\tau - d_{\rm min}$ contour diagram. Also given are the neutron star parameters needed as well as the position of the potential SN.

[5]We find additional small separations for Bochum 13 and NGC 6383; however, the fraction of such runs is very small.

It has been previously suggested that RX J0720.4−3125 originated from the Trumpler 10 (Tr 10) association by Motch, Zavlin & Haberl (2003) who considered the general direction of the neutron star's motion and Kaplan, van Kerkwijk & Anderson (2007) who investigated the probability of close approaches of the neutron star to any of the OB associations given in de Zeeuw et al. (1999) giving the proper motion randomly directions and sign as well as varying the radial velocity in a certain range and adopting specified distances. They concluded that it is very likely that Tr 10 is the birth place. Since early B-type stars are present in Tr 10, it is plausible that the association already experienced a SN. Varying the parallax in the range $\pi \pm \sigma_\pi$ and the radial velocity in the range $v_{\rm r} \pm 0.935 v_{\rm t}$ (0.935 corresponds to 1σ in $v_{\rm r}$ for random orientation, $v_{\rm t}$ is the transverse velocity), Kaplan et al. (2007) found a separation between the neutron star and the centre of Tr 10 of 17 pc 0.7 Myr ago for a radial velocity of −20 to +50 km s^{-1}. Infact, we find the smallest separation between RX J0720.4−3125 and the centre of Tr 10 to be 17 pc $\approx$0.6 Myr in the past. We find radial velocities in the range of −50 to 500 km s^{-1} for which RX J0720.4−3125 would have come as close as 30 pc to the centre of Tr 10. In the $\tau - d_{\rm min}$ contour plot a maximum lies at $d_{\rm min}$ between 23 and 40 pc and corresponding flight times τ of 0.44 and 0.65 Myr. The slope of the histogram of minimum separations $d_{\rm min}$ within this time range [Fig. 5(c)] is in good agreement with a 3D Gaussian implying $d_{\rm min} = 33.0 \pm 2.8$ pc. Given a radius of Tr 10 of 23 pc, this means that the potential SN would have occurred outside the association or, if we relax the boundary condition, at least at its outer edge making the scenario less likely [the probability is two times smaller than for TW Hydrae (TWA)]. If we nevertheless adopt Tr 10 as the birth place of RX J0720.4−3125 (Fig. 6) and consider the association age (15– 35 Myr), we estimate a progenitor mass of $\approx$7–13 $M_\odot$ (models from T80, MM89 and K97), corresponding to a spectral type between B4 and B1 on the main sequence (Schmidt-Kaler 1982). Motch et al. (2003) and Kaplan et al. (2007) also suggest Vela OB2 (Vel OB2) as a possible birth place of RX J0720.4−3125 for which we find a minimum separation of 81.6 pc (cf. 70 pc stated by Kaplan et al. 2007) which is outside the association with a radius of 35 pc.

We exclude Pup OB3 as birth association owing to a very small parallax needed to reach the association implying a current distance to the Sun of >1 kpc. For that reason, the probability of Pup OB3 being the birth site of RX J0720.4−3125 is more than five times smaller than for TWA (and more than two times for most of the other associations listed in Table 6).

The four other associations for which we find a maximum in the $\tau - d_{\rm min}$ contour plot which is located well within the association boundaries are YLA – TWA, Tucana/Horologium (Tuc-Hor), the β Pictoris moving group (β Pic-Cap) and HD 141569. For two of them, TWA and the HD 141569 group, the smallest separation between RX J0720.4−3125 and the centre of the particular association is smaller than 5 pc. For that reason, it seems plausible that one of those two may be the birth place of RX J0720.4−3125. However, since the radii of Tuc-Hor (50 pc) and β Pic-Cap (56 pc) are rather large, they could also have hosted the SN. Compared to TWA the probabilities that one of those two associations hosted the SN which formed RX J0720.4−3125 is 2–3 times smaller.

Figs 5(a) and (b) show the distributions of minimum separations $d_{\rm min}$ to the centres of TWA and HD 141569. From the theoretical curves, we can predict that a potential SN which formed RX J0720.4−3125 in HD 141569 would have been situated 15 ± 2 pc from the centre, i.e. at the edge of the association with a radius of about 15 pc. Moreover, since HD 141569 only consists of five members (F08), it is rather unlikely to have hosted a SN far from

Table 6. Potential parent associations of RX J0720.4−3125, columns as in Table 4.

Association	$d_{\rm min}$ (pc)	τ (Myr)	$v_{\rm r}$ (km s^{-1})	μ_{α^*} (mas yr^{-1})	μ_δ (mas yr^{-1})	$v_{\rm space}$ (km s^{-1})	π (mas)	$\rm d_\odot$ (pc)	α (°)	δ (°)
TWA	0...12	0.34...0.46	502^{+111}_{-88}	-93.9 ± 2.2	52.8 ± 2.3	518^{+112}_{-90}	$4.06^{+0.47}_{-0.49}$	48...67	$187.10^{+3.44}_{-2.91}$	$-37.98^{+1.53}_{-1.38}$
Tuc-Hor	44...80	0.26...0.52	476^{+128}_{-73}	-93.8 ± 2.2	52.8 ± 2.3	492^{+129}_{-75}	$4.12^{+0.55}_{-0.47}$	35...70	$190.19^{+4.00}_{-4.97}$	$-37.29^{+1.30}_{-1.44}$
β Pic-Cap	35...84	0.31...0.61	468^{+106}_{-87}	-93.9 ± 2.2	52.8 ± 2.3	486^{+107}_{-89}	$3.94^{+0.53}_{-0.39}$	38...78	$209.87^{+3.13}_{-3.20}$	$-28.52^{+2.04}_{-2.15}$
HD 141569	12...22	0.52...0.75	469^{+108}_{-70}	-93.8 ± 2.2	53.0 ± 2.3	488^{+111}_{-73}	$3.80^{+0.56}_{-0.55}$	96...116	240...250	−6...3
Pup OB3	14...42	0.47...0.61	-375^{+144}_{-150}	-94.0 ± 2.1	52.9 ± 2.3	715^{+143}_{-110}	$0.84^{+0.05}_{-0.05}$	1440^{+12}_{-23}	$124.11^{+1.27}_{-0.60}$	$-37.16^{+0.43}_{-0.35}$
Tr 10	23...40	0.44...0.65	290^{+143}_{-110}	-93.8 ± 2.2	53.1 ± 2.2	393^{+136}_{-102}	$1.93^{+0.24}_{-0.20}$	335...375	135...140	$-40.19^{+0.58}_{-0.59}$

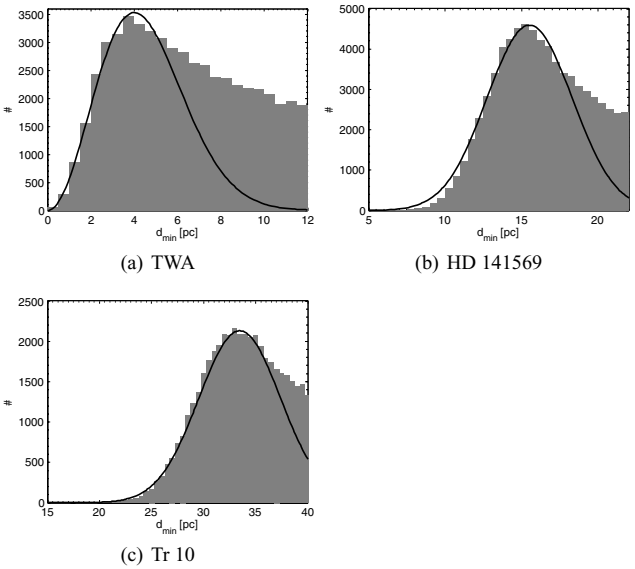

Figure 5. (a) Distribution of minimum separations $d_{\rm min}$ between RX J0720.4−3125 and the centres of TWA (a), HD 141569 (b) and Tr 10 (c), respectively, within the defined time range τ (see Table 6, Column 3). Shown as well are theoretical curves for 3D Gaussian distributions (equation 1) with $\mu = 0$ pc and $\sigma = 2$ pc for TWA, $\mu = 15$ pc and $\sigma = 2$ pc for HD 141569 and $\mu = 33$ pc and $\sigma = 2.8$ pc for Tr 10. Note that the curves are not fitted to the data (see also Fig. 3).

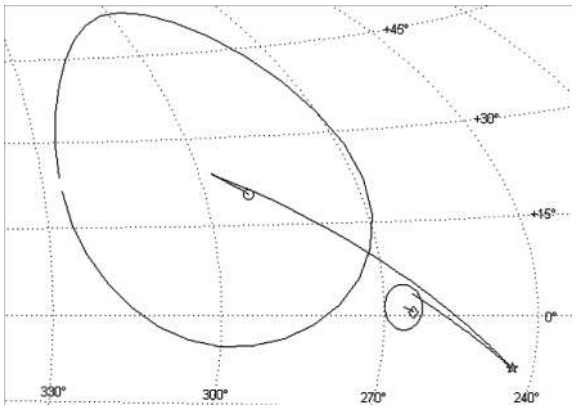

Figure 6. Past trajectories for RX J0720.4−3125 and Tr 10 and TWA, respectively, projected on a Galactic coordinate system (for particular sets of input parameters consistent with Table 6). Present positions are marked with a star for the neutron star and a diamond for Tr 10 and an open circle for TWA. Large circles reflect association extensions (radii of 23 pc for Tr 10 and 33 pc for TWA).

its core. The probability of such a scenario is seven times smaller than for TWA.

In the case of TWA, we can predict the SN very close to the association centre at a separation of 0 ± 2 pc. Then, RX J0720.4−3125 would have been formed ≈0.4 Myr ago and its current radial velocity would be ≈500 km s^{-1} (space velocity ≈520 km s^{-1}). The current distance to the Sun which the neutron star would have in this case is ≈250 pc which is in very good agreement with 235–265 pc as derived by Posselt et al. (2007) (thereafter P07) from the spectrum and $n_{\rm H}$ (note that they obtained a slightly higher value of 1.2×10^{20} cm^{-2} compared to the most recent value from Hohle et al. 2009; Table 2) as well as with the parallax of 2.77 ± 1.29 mas (Kaplan et al. 2007).

The potential SN would have occurred between 48 and 67 pc from the Sun. For such a small distance, we expect to find SN-produced radionuclides in the terrestrial crust (Ellis, Fields & Schramm 1996) such as ^{10}Be and ^{60}Fe, with half-lives of 1.5 Myr (Acton et al. 1993) and 2.6 Myr (Rugel et al. 2009), respectively. A small but insignificant signal of ^{60}Fe was found at a time below 1 Myr (Knie et al. 2004; Fitoussi et al. 2008). For ^{10}Be anomalous abundances in Antarctic ice cores corresponding to times of ≈0.35 and ≈0.6 Myr in the past were identified (Raisbeck et al. 1987). The first signal has also been reported for deep-sea sediments in the Gulf of California (McHargue, Damon & Donahue 1995) and in the Mediterranean (Cini Castagnoli et al. 1995). More recently, Cole et al. (2006) analysed ice cores from the Qinghai–Tibetan plateau in China but could not confirm previous findings. However, it seems possible that a recent SN in TWA which produced RX J0720.4−3125 (Fig. 6) contributed to one of the ^{10}Be signals.

Moreover, F08 state that it is likely that one or more of the YLA hosted a SN in the near past. Despite the small number of TWA members, we can expect one 10 $\rm M_\odot$ star to have been born in TWA due to its present mass function[6] (Fig. 7). Given the association age of 3–20 Myr (e.g. Barrado Y Navascués 2006), we estimate a progenitor mass of 10 (B2V) up to 100 $\rm M_\odot$ (O4V) (10 to >50 $\rm M_\odot$ for T80, 11–100 $\rm M_\odot$ for MM89 and 10– 100 $\rm M_\odot$ for K97; spectral types from Schmidt-Kaler 1982).

If RX J0720.4−3125 was born in TWA, the SN would have contributed only a small amount to ^{10}Be and ^{60}Fe found in the Earth's crust due to the relatively low-mass progenitor (≈10 $\rm M_\odot$). This would be consistent with the findings. Furthermore, we propose a larger age (≈20 Myr) for TWA.

[6]We estimated the masses for the TWA members listed in F08, taking also into account that HD 98800 (Soderblom et al. 1998) and TWA-5 (Neuhäuser et al. 2000a; Torres et al. 2003) are both quadruple, using the D'Antona & Mazzitelli (1997) model, and 2.9 $\rm M_\odot$ for the A0-type main-sequence star HR 4796 A.

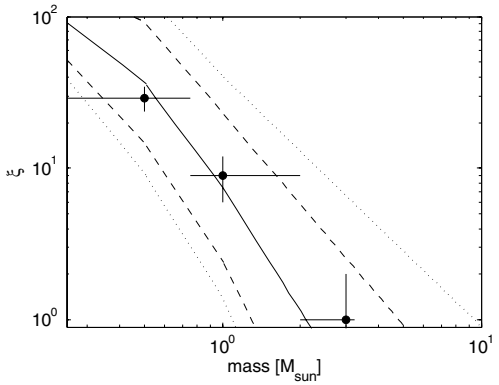

Figure 7. Present TWA mass function (black circles, see footnote 6) in comparison with the initial mass function ξ (IMF, solid line) as given by Kroupa & Weidner (2005), their equation (2). Dashed and dotted lines represent the 1 and 1.5σ IMF boundaries. Within 1.5σ, we expect up to one star with 10 $M_\odot$; the probability for higher mass stars is low.

Table 7. Associations for which the smallest separation between RX J1605.3 + 3249 and the association centre found (min. $d_{\rm min}$) after 2 million runs was within the radius of the association, as Table 3.

Association	min. $d_{\rm min}$ (pc)	R_{Assoc} (pc)
US	4.6	15
UCL	13.0	33
Tuc-Hor	5.2	50
β Pic-Cap	6.3	57
ϵ Cha	21.4	28
HD 141569	9.1	16
Ext. R CrA	25.3	31
AB Dor	12.7	43
NGC 6322	2.2	11
Bochum 13	2.1	2
Sco OB4	0.9	33

5.3 RX J1605.3+3249

Since there is currently only an upper limit of the distance (<410 pc, Motch et al. 2007) available for RX J1605.3 + 3249, thus a lower limit for the parallax ($\pi > 2.4$ mas, see Table 2) we had to adopt a value for our investigations. The hydrogen column density of $n_{\rm H} = 1.1 \pm 0.4 \times 10^{20}$ cm^{-2} (Motch et al. 1999) predicts a relatively small distance of RX J1605.3 + 3249 to the Sun. For that reason, we chose a parallax value of $\pi = 5 \pm 3$ mas corresponding to a distance of 200^{+300}_{-75} pc. Infact, this is a source of large uncertainty. After the 2 million run investigation, we identify 11 associations for which the smallest separation $d_{\rm min}$ between the association centre and RX J1605.3 + 3249 was consistent with the association radius (Table 7). Five of them show a maximum in the $\tau - d_{\rm min}$ contour plot also being consistent with the respective association boundaries (Table 8, top).

Due to the small parallax needed for RX J1605.3 + 3249 to reach the Scorpius OB4 (Sco OB4) association ($\pi = 1.1$ mas, Column 7 of Table 8), we may exclude this association since this is even smaller than the lower limit of $\pi > 2.4$ mas (Table 2).

The remaining four associations once again belong to the YLA (F08). We can explain the slopes of the histograms of minimum separations $d_{\rm min}$ with 3D Gaussians (equation 1) that predict the place of the potential SN within the boundaries of the associations (see Fig. 8). For the YLA, the simulations suggest a very small current distance of the neutron star to the Sun between 100 and 250 pc. From $n_{\rm H}$ P07 derived a distance between 325 and 390 pc [they obtained $n_{\rm H} = 2.0 \times 10^{20}$ cm^{-2} without giving errors; however, for an $n_{\rm H}$ of $\approx 1 \times 10^{20}$ cm^{-2} (Table 2), the distance should at least be $\approx$230 pc, cf. P07 their table 2]. For that reason, we find Tuc-Hor, β Pic-Cap and AB Dor to be less likely parent associations of RX J1605.3 + 3249 since the neutron star would then need to have a current distance to the Sun smaller than 160 pc.[7]

In Table 8 (bottom), we also give the results for two associations of the Scorpius-Centaurus (Sco-Cen) complex – US and Upper Centaurus Lupus (UCL) – for which slightly larger distances are required. Constraining the age to 1 Myr as a maximum and using current distances of 100– 500 pc as well as radial velocities in the range of ± 700 km s^{-1}, Motch et al. (2005) proposed the origin of RX J1605.3 + 3249 in US. We consider the Sco-Cen complex also to be a likely birth site of RX J1605.3 + 3249. The respective $d_{\rm min}$ histograms are shown in Figs 8(e) and (f).

Hence, we conclude that RX J1605.3 + 3249 either originated from the extended Corona–Australis association $\approx$0.5 Myr ago with a current distance of $\approx$230 pc and radial velocity of $\approx$320 km s^{-1} (space velocity $\approx$360 km s^{-1}) or was born in the Sco-Cen complex 28.5 $\pm$ 2.0 pc from the centre of US about 0.5 Myr in the past (Fig. 9). The first scenario is possible due to the existence of B-type stars (highest content within the YLA, F08), thus late O- or early B-type stars may have been born there. For the latter scenario, the current distance to the Sun would be $\approx$300 pc and the neutron star's radial velocity $\approx$340 km s^{-1} (space velocity $\approx$400 km s^{-1}). Both the cases would be in good agreement with a space velocity of $\approx$400 km s^{-1}, which reflects the mean velocity of the velocity distribution for pulsars from Ho05.

Accepting one of the two birth sites and taking the ages of the associations of 5– 10 Myr (US) and 10–15 Myr (Ext. R CrA), we estimate the mass of the progenitor star to be 17 (B0V) to 45 $M_\odot$ (O5.5V) (29–45 $M_\odot$ for T80, 18–42 $M_\odot$ for MM89, 17–36 $M_\odot$ for K97) for a birth in the Sco-Cen complex or 12 (B1V) to 30 $M_\odot$ (O7V) (13–30 $M_\odot$ for T80, 13–18 $M_\odot$ for MM89, 12–17 $M_\odot$ for K97) for a birth in Ext. R CrA (spectral types from Schmidt-Kaler 1982).

Such a nearby SN (see Table 8, Column 8) could also have contributed to the ^{10}Be and ^{60}Fe material found in the Earth's crust (e.g. Raisbeck et al. 1987; Knie et al. 2004).

5.4 RBS 1223 (RX J1308.8+2127)

For RBS 1223 both distance limits are available (76–700 pc, Schwope et al. 2005; Motch et al. 2007, hence $\pi = 1.4$–13 mas). Since the span between those limits is rather large, we adopted a parallax of $\pi = 7 \pm 5$ mas which is, as for RX J1605.3 + 3249, a source of large uncertainty. After performing 2 million Monte Carlo runs, we found 22 associations for which the smallest separation between RBS 1223 and the association centre found was within the association radius (Table 9). Five of these 23 show well-defined areas of higher probability in their $\tau - d_{\rm min}$ contour plots (Table 10), whereas for more distant (> 1 kpc) associations as well as Serpens OB1 (Ser OB1) and M6 (below Her-Lyr in Table 9) only very few runs yield small separations $d_{\rm min}$ between the neutron star and the association centre. The latter behaviour does not change even if we constrain input parallaxes to a range of 3 ± 2 mas. Furthermore, an

[7]Estimating probabilities, even rough values, is unreliable in the case of RX J1605.3+3249 because of the uncertain distance. Hence, an individual discussion is appropriate.

Table 8. Potential parent associations of RX J1605.3+3349, columns as in Table 4.

Association	$d_{\rm min}$ (pc)	τ (Myr)	$v_{\rm r}$ (km s^{-1})	μ_{α^*} (mas yr^{-1})	μ_δ (mas yr^{-1})	$v_{\rm space}$ (km s^{-1})	π (mas)	$d_\odot$ (pc)	α (°)	δ (°)
Tuc-Hor	7...15	0.24...0.39	452^{+115}_{-76}	-43.7 ± 1.7	148.7 ± 2.6	462^{+118}_{-78}	$7.54^{+1.53}_{-1.33}$	39^{+5}_{-4}	$32.48^{+10.60}_{-34.55}$	$-75.69^{+4.70}_{-1.55}$
β Pic-Cap	8...10	0.16...0.24	537^{+103}_{-93}	-43.7 ± 1.7	148.6 ± 2.6	543^{+104}_{-94}	$8.86^{+1.60}_{-1.09}$	18^{+2}_{-7}	$292.49^{+13.51}_{-22.49}$	$-75.21^{+8.25}_{-1.41}$
Ext. R CrA	30...42	0.43...0.64	321^{+109}_{-58}	-43.7 ± 1.7	148.8 ± 2.6	362^{+117}_{-66}	$4.41^{+0.90}_{-0.85}$	70...115	$261.99^{+1.12}_{-0.99}$	$-39.84^{+2.10}_{-2.00}$
AB Dor	21...43	0.17...0.32	452^{+109}_{-84}	-43.7 ± 1.7	148.7 ± 2.6	462^{+110}_{-85}	$7.56^{+1.22}_{-0.78}$	21^{+7}_{-6}	$264.30^{+4.76}_{-4.93}$	$-44.11^{+6.98}_{-8.82}$
Sco OB4	12...74	1.28...1.68	311^{+75}_{-69}	-43.7 ± 1.7	148.7 ± 2.6	743^{+98}_{-77}	$1.09^{+0.08}_{-0.08}$	1042...1140	$259.57^{+0.97}_{-0.99}$	$-35.0... - 30.5$
US	26...36	0.46...0.63	343^{+86}_{-80}	-43.7 ± 1.6	148.8 ± 2.6	406^{+92}_{-85}	$3.38^{+0.47}_{-0.41}$	129...171	$255.09^{+0.57}_{-0.66}$	$-18.44^{+1.00}_{-1.06}$
UCL	50...63	0.48...0.73	318^{+116}_{-63}	-43.7 ± 1.7	148.7 ± 2.6	375^{+122}_{-72}	$3.70^{+0.71}_{-0.59}$	96...164	$260.48^{+0.81}_{-0.86}$	$-35.68^{+1.83}_{-1.60}$

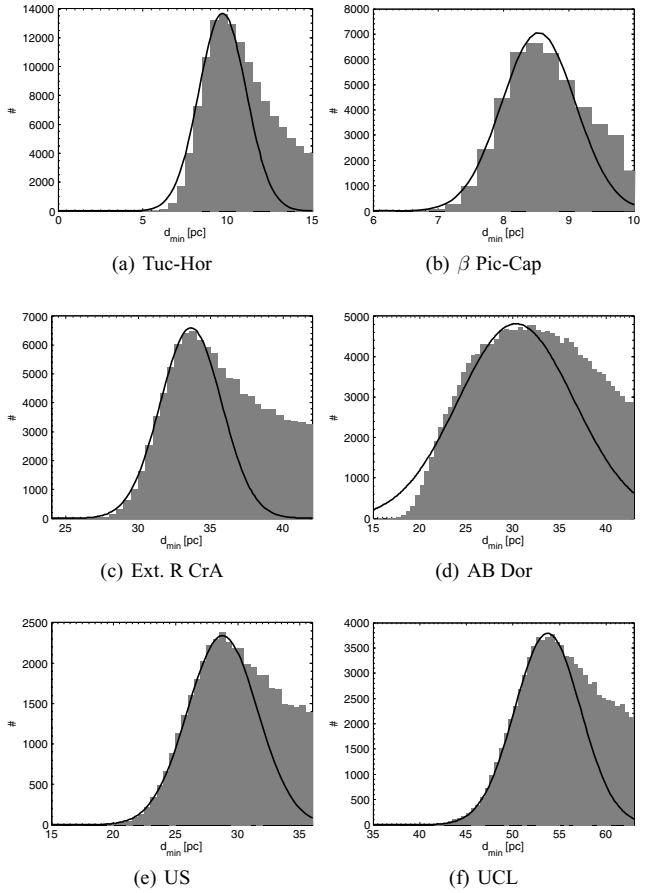

Figure 8. (a) Distribution of minimum separations $d_{\rm min}$ between RX J1605.3 + 3249 and the centres of Tuc-Hor (a), β Pic-Cap (b), Ext. R CrA (c), AB Dor (d), US (e) and UCL (f), respectively, within the defined time range τ (see Table 8, Column 3). Shown as well are theoretical curves for three-dimensional Gaussian distributions (equation 1) with $\mu = 9.5$ pc and $\sigma = 1.0$ pc for Tuc-Hor, $\mu = 8.5$ pc and $\sigma = 0.4$ pc for β Pic-Cap, $\mu = 33.5$ pc and $\sigma = 1.5$ pc for Ext. R CrA, $\mu = 29.0$ pc and $\sigma = 4.5$ pc for AB Dor, $\mu = 28.5$ pc and $\sigma = 2.0$ pc for US and $\mu = 53.5$ pc and $\sigma = 2.5$ pc for UCL. Note that the curves are not fitted to the data (see also Fig. 3).

origin in most of those associations implies a parallax smaller than the lower limit of 1.4 mas. For those reasons, we may exclude them as probable birth associations for RBS 1223.

However, calculating past trajectories of RBS 1223, Motch et al. (2007) proposed that a small fraction of orbits passes though the Scutum OB2 (Sct OB2) association. More recently, Motch et al. (2009) reinvestigated this association considering that it consists of two groups, Sct OB2A at 510 pc and Sct OB2B at 1170 pc (Reichen

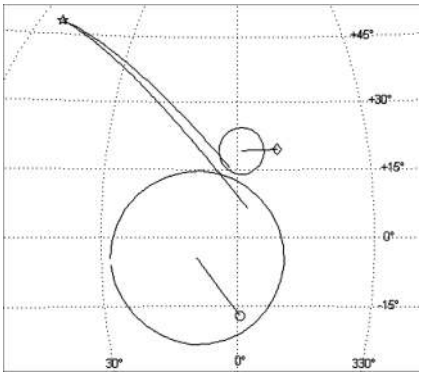

Figure 9. Past trajectories for RX J1605.3 + 3249 and US and Ext. R CrA, respectively, projected on a Galactic coordinate system (for particular sets of input parameters consistent with Table 8). Present positions are marked with a star for the neutron star and a diamond for US and an open circle for Ext. R CrA. Large circles reflect association extensions (radii of 15 pc for US and 31 pc for Ext. R CrA).

et al. 1990). We adopt these two distances and the proper motion and radial velocity for Sct OB2 from Dambis et al. (2001) and calculate again 2 million orbits for both, the neutron star and each subgroup, as well as their separations $d_{\rm min}$ at each time-step τ. Due to the large uncertainty in parallax and radial velocity of RBS 1223, we do not find a maximum in their $\tau - d_{\rm min}$ plots, but can derive flight time ranges from the τ histograms for which smaller separations ($d_{\rm min} \leq 50$ pc) occur. Considering the input parameters of the runs in the derived time ranges, we obtain the neutron star properties and potential SN positions as given in Table 11.

All associations for which we found a peak in their $\tau - d_{\rm min}$ contour plot that was consistent with the association boundaries (Table 10, top) belong to the YLA (F08) and imply a rather small present distance of RBS 1223 to the Sun. Regarding the hydrogen column density of $n_{\rm H} = 1.8 \pm 0.2 \times 10^{20}$ cm^{-2} (Schwope et al. 2007) which is comparable to other M7 members and even a bit higher (see Table 2), the distance of RBS 1223 to the Sun is supposed to be at least 180 pc (the distance to the Sun of the probably closest member RX J1856.5-3754 is ≈180 pc), corresponding to a parallax smaller than approximately 5.5 mas. For that reason, we can exclude three of the YLA – Tuc-Hor, β Pic-Cap and AB Dor – for which the current distance to RBS 1223 would be smaller than 100 pc.[8] From the $\tau - d_{\rm min}$ contour plot for HD 141569, a potential SN in HD 141569 would have occurred near the edge of the group our

[8] As for RX J1605.3 + 3249, the distance of RBS 1223 is too poorly known to estimate probabilities for the potential parent associations. For that reason, we give an individual discussion.

Table 9. Associations for which the smallest separation between RBS 1223 and the association centre found (min. $d_{\rm min}$) after 2 million runs was within the radius of the association, as Table 3.

Association	min. $d_{\rm min}$ (pc)	$R_{\rm Assoc}$ (pc)
US	1.1	15
Tuc-Hor	10.3	50
β Pic-Cap	0.3	57
HD 141569	0.1	16
Ext. R CrA	0.3	31
AB Dor	7.9	43
Her-Lyr	9.7	13
Sgr OB5	6.2	111
NGC 6530	1.3	6
Sgr OB1	2.2	104
Sgr OB7	3.0	29
Sgr OB4	5.0	27
Sgr OB6	1.8	17
M 17	3.5	10
Ser OB1	1.1	36
NGC 6611	0.8	7
Sct OB3	2.2	17
Ser OB2	3.7	31
NGC 6604	4.5	8
Sct OB2	6.6	31
NGC 6383	3.0	5
M6	2.5	4

even outside (between 5 and 21 pc, the radius of HD 141569 is $\approx$16 pc) and thus is unlikely.

Indeed, the case Ext. R CrA is very promising, since the shape of the $d_{\rm min}$ distribution is in good agreement with a 3D Gaussian distribution with $\mu = 0$ and $\sigma = 13.5$ [see Fig. 10(a), equation 2]. Hence, a potential SN which created RBS 1223 would have occurred near the centre of the association. Assuming this, RBS 1223 would now be $\approx$0.5 Myr old. Its current radial velocity would be $\approx$350 km s^{-1} (space velocity $\approx$400 km s^{-1}). Furthermore, it is very likely that Ext. R CrA experienced a SN in the near past owing to the existence of B-type stars (highest content within the YLA, F08).

In Table 10 (bottom), we also give the results for the US association which has also been suggested as a possible birth place for RBS 1223 by Motch et al. (2009). Although the $d_{\rm min}$ histogram in this case does not support a birth in US [a SN is predicted at a distance from the US centre of 51 ± 12 pc, see Fig. 10(b)], it seems possible that the neutron star was born in the Sco-Cen complex (similar to RX J1605.3 + 3249, see previous section) in the vicinity of US. In this case, the present distance of RBS 1223 to the Sun would be slightly larger as for Ext. R CrA ($\approx$215 pc) whereas age and radial velocity are similar to those for Ext. R CrA ($\tau \approx 0.5$ Myr, $v_{\rm r}$ $\approx$350 km s^{-1}, space velocity $\approx$420 km s^{-1}). Adopting a near birth scenario either in the Sco-Cen complex or Ext. R CrA 0.5 Myr ago (Fig. 11), we can estimate the mass of the progenitor of RBS 1223. Given association ages of 5–10 Myr for US and 10–15 Myr for Ext. R CrA, the mass would be 17 (B0V) to 45 $M_\odot$ (O5.5V) (US) or 12 (B1V) to 30 $M_\odot$ (O7V) (Ext. R CrA) (T80; MM89; K97; spectral types from Schmidt-Kaler 1982).

However, since the distance to RBS 1223 is very uncertain and following P07 can only hardly get constrained through $n_{\rm H}$, we eventually cannot completely exclude the associations in the lower part of Table 9. Infact, in the case RBS 1223, P07 reached the limit of their modelling which was set at 1 kpc. Thus, the neutron star might be located at somewhat larger distances which would be consistent with its origin lying in the Sct region. If so, we can again estimate the mass of the progenitor star adopting an age of RBS 1223 of 1 Myr (Fig. 11) and Sct OB2 of 6 Myr (Schild & Maeder 1985). Models from T80, MM89 and K97 yield masses of 44, 38 and 32 $M_\odot$ ($\approx$O6 on the main sequence).

5.5 Remarks

It has to be mentioned that any association identified for which it is possible to trace our neutron stars back such that they reach the association boundary (although it might be only fulfilled for a very small fraction of runs) is a potential parent association. However, for a few associations, theoretical curves (equations 1 and 2) fit the $d_{\rm min}$ histograms remarkably well. Hence, we conclude that they reflect the real separation at the encounter time (flight time).

Furthermore, it is important to bear in mind that the initially input distribution for radial velocities (Ho05) somewhat biases the outcoming radial velocities to median ranged values ($\approx\pm$400 km s^{-1}, depending on the transverse velocity). Due to this bias, the range of τ (flight time) might be underestimated. None the less, our method allows us to also identify associations requiring either very small or high radial velocities.

Compared to previous investigations of the origin of M7 members as done by e.g. Walter & Lattimer (2002), Motch et al. (2003), Kaplan et al. (2007) and Motch et al. (2009), our calculations do not only cover certain radial velocity ranges, but the whole spectrum of possible radial velocities ranging from -1500 to $+1500$ km s^{-1}. To account for the velocity distribution for neutron stars, we used the probability distribution of Ho05. Furthermore, we vary the distances for RX J1605.3 + 3249 and RBS 1223 in a wide range to account for their large uncertainties.

We compiled a list of 140 OB associations and clusters to cover most[9] of the potential birth sites of neutron stars.

For estimating the SN progenitor star mass from the difference between association age and kinematic age, we assumed that all stars formed about at the same time in that association. This assumption is justified because once an O or B star is formed, its strong wind and slightly later its SN shock front will blow away all the remaining gas, so that star formation will cease in that region. This assumption holds for OB associations and is consistent with observations. It does not necessary hold for associations without an O- or B-type star, like possibly TWA, which however may have had an early B-type star.

6 CONCLUSIONS

We reviewed the prominent neutron star/ runaway case PSR B1929 + 10/ ζ Oph (H01) and re-investigated it with more recent data for the pulsar. Although we did not put constraints on the radial velocity, we could confirm previous results from Bobylev (2008) and eventually derive a radial velocity of $\approx$250 km s^{-1} of the pulsar which is needed to find the two objects at nearly the same position in US at the same time in the past. However, we should bear in mind that we had to increase the errors of the parallax and proper motion components. If they are truly as small as published by Chatterjee et al. (2004) the scenario is less likely.

We investigated the motion of four members of the M7 and for each neutron star simultaneously the motion of 140 OB associations and clusters to confine potential parent associations of the neutron stars. A summary of our results is given in Table 12 (for individual discussions please see previous sections).

[9]However, some neutron stars may have been former massive runaway stars.

Table 10. Potential parent associations of RBS 1223, columns as in Table 4.

Association	$d_{\rm min}$ (pc)	τ (Myr)	$v_{\rm r}$ (km s^{-1})	μ_{α^*} (mas yr^{-1})	μ_δ (mas yr^{-1})	$v_{\rm space}$ (km s^{-1})	π (mas)	$d_\odot$ (pc)	α (°)	δ (°)
Tuc-Hor	23...30	0.17...0.31	463^{+94}_{+82}	-206 ± 19	84 ± 18	473^{+100}_{-86}	$10.85^{+3.38}_{-2.16}$	37^{+4}_{-3}	$339.68^{+14.32}_{-9.68}$	$-29.20^{+2.56}_{-3.33}$
β Pic-Cap	5...10	0.13...0.22	482^{+106}_{-95}	-206 ± 19	82 ± 19	490^{+110}_{-98}	$12.06^{+2.45}_{-2.25}$	19^{+2}_{-3}	$316.23^{+11.81}_{-7.80}$	$-29.63^{+3.70}_{-3.90}$
HD 141569	5...21	0.27...0.40	332^{+103}_{-85}	-209 ± 19	85 ± 20	393^{+130}_{-99}	$5.09^{+0.91}_{-0.98}$	84...122	$236.46^{+7.70}_{-9.09}$	$1.55^{+5.55}_{-4.74}$
Ext. R CrA	16...40	0.38...0.58	345^{+114}_{-90}	-209 ± 20	85 ± 18	391^{+137}_{-103}	$5.78^{+1.33}_{-1.21}$	80^{+22}_{-10}	$294.82^{+7.24}_{-7.92}$	$-22.94^{+4.33}_{-6.29}$
AB Dor	15...28	0.15...0.24	437^{+99}_{-95}	-206 ± 20	83 ± 19	446^{+104}_{-97}	$11.56^{+2.24}_{-2.05}$	18^{+4}_{-3}	225...358	$-28.86^{+11.77}_{-6.85}$
US	42...64	0.38...0.55	351^{+100}_{-104}	-210 ± 20	83 ± 18	420^{+154}_{-118}	$4.63^{+0.84}_{-1.27}$	109^{+36}_{-19}	$254.09^{+2.11}_{-2.34}$	$-6.29^{+3.23}_{-5.09}$

Table 11. Results for RBS 1223 and Sct OB2A and B. Minimum separations have been constrained to $d_{\rm min} \leq 50$ pc. Column 2 gives the smallest separation $d_{\rm min}$ found after 2 million runs, Column 3 gives the maximum of the time (τ) histogram along with its 68 per cent interval (note that this is not a 1σ error). Columns 4–10 indicate the current neutron star properties needed to yield small separations to the particular association as well as the position of the potential SN (see also Table 4). Note that receding radial velocities are positive contrary to Motch et al. (2009).

Association	min. $d_{\rm min}$ (pc)	τ (Myr)	$v_{\rm r}$ (km s^{-1})	μ_{α^*} (mas yr^{-1})	μ_δ (mas yr^{-1})	$v_{\rm space}$ (km s^{-1})	π (mas)	$d_\odot$ (pc)	α (°)	δ (°)
Sct OB2A	1.6	$1.07^{+0.56}_{-0.34}$	75...310	-216 ± 19	53 ± 10	272...597	$2.70^{+0.96}_{-0.44}$	517^{+18}_{-19}	$277.15^{2.47}_{2.60}$	$-12.04^{+2.13}_{-1.83}$
Sct OB2B	3.2	$1.56^{+0.80}_{-0.42}$	285^{+107}_{-129}	-221 ± 20	46 ± 7	731^{+313}_{-172}	$1.59^{+0.22}_{-0.38}$	1199^{+19}_{-19}	$277.93^{+1.22}_{-1.41}$	$-10.12^{+1.93}_{-0.63}$

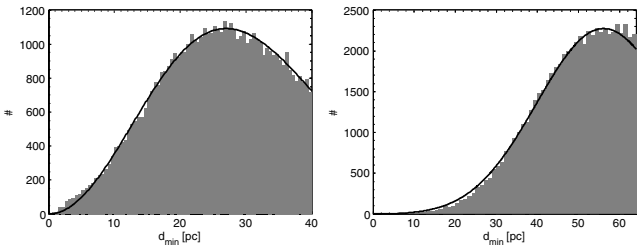

(a) Ext. R CrA (b) US

Figure 10. Distribution of minimum separations $d_{\rm min}$ between RBS 1223 and the centre of the extended Corona–Australis association (a) and US (b) within the defined time range τ (see Table 10, Column 3). Shown as well is a theoretical curve for a 3D Gaussian distributions (equations 1 and 2) with $\mu = 0$ pc and $\sigma = 13.5$ pc for Ext. R CrA and $\mu = 51$ pc and $\sigma = 12$ pc for US. Note that the curves are not fitted to the data but will just give an explanation of the slopes of the histograms.

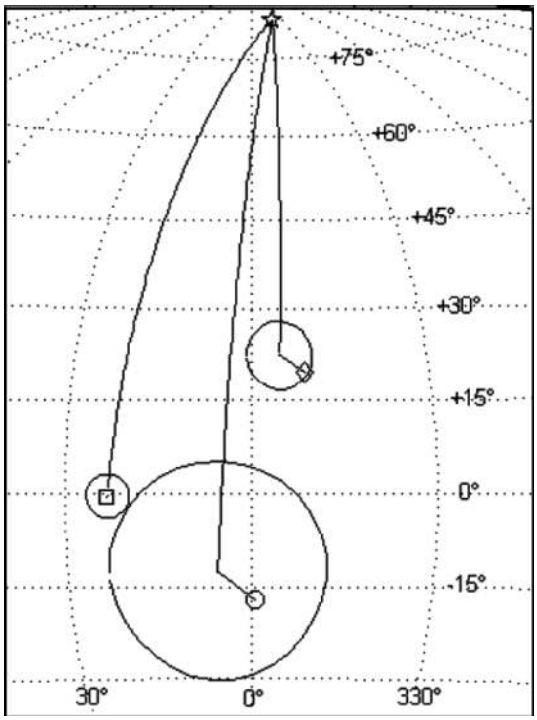

Figure 11. Past trajectories for RBS 1223 and US, Ext. R CrA and Sct OB2, respectively, projected on a Galactic coordinate system (for a particular set of input parameters consistent with Table 10). Present positions are marked with a star for the neutron star, a diamond for US, an open circle for Ext. R CrA and a square for Sct OB2. Large circles reflect association extensions (radii of 15 pc for US, 31 pc for Ext. R CrA) and 31 pc for Sct OB2.

We find that RX J1856.5−3754 most probably originated from US about 0.3 Myr ago. RX J0720.4−3125 was very likely born in TWA about 0.4 Myr ago or may come from Tr 10, where the SN then would have occurred 0.5 Myr in the past. RX J1605.3 + 3249 and RBS 1223 also were seemingly born from a close young association such as the Sco-Cen complex or Ext. R CrA. For RBS 1223 also a birth in Scutum OB2 is possible.

Thus, we find that the most probable birth places were located close to the Sun. The SN distances are consistent with the local bubble and hence may have contributed to its formation or reheating (Berghöfer & Breitschwerdt 2002; F08). There is no doubt that the Sco OB2 association to which US belongs experienced some SNe in the past (Maíz-Apellániz 2001; Berghöfer & Breitschwerdt 2002; F08). There have been other investigations showing that many neutron stars may have been born within the Gould Belt (Popov et al. 2003), a torus-like structure around the Sun with a radius of ≈600 pc (Torra, Fernández & Figueras 2000), to which most of the associations just mentioned also belong.

Some of the four investigated M7 neutron stars may have formed within ≈250 pc within the last 0.5 Myr, so that they could have contributed to the ^{10}Be and ^{60}Fe found in the Earth's crust.

Adopting a birth scenario of each neutron star, we can derive estimations of the mass of the progenitor star assuming contemporary star formation in the association as well as the kinematic neutron star age which we here always find to be lower than the

Table 12. Summary of the results discussed in Section 5. Given here are those associations that we conclude to be the most probable birth places of the four M7 members. Columns 3–5 give the position of the potential SN as equatorial coordinates and distance to the Sun, Column 6 gives the approximate time in the past at which the SN may have occurred and Columns 7–10 give constraints on the neutron star parameters as they would be needed to reach the respective association at the given time.

RX J	Association	Position of SN			Time	Present-day parameters			
		$\alpha(^\circ)$	$\delta(^\circ)$	$d_\odot$(pc)	of SN	π(mas)	v_T (km s^{-1})	$\mu\alpha^*$ (mas yr^{-1})	$\mu\delta$ (mas yr^{-1})
1856.5-3754	US	$243.21^{+0.58}_{-0.52}$	$-23.66^{+0.31}_{-0.29}$	140...163	0.3 Myr	$5.41^{+0.33}_{-0.28}$	193^{+45}_{-32}	326.7 ± 0.8	-59.1 ± 0.7
0720.4-3125	TWA	$187.10^{+3.44}_{-2.91}$	$-37.98^{+1.53}_{-1.38}$	48...67	0.4 Myr	$4.06^{+0.47}_{-0.49}$	502^{+111}_{-88}	-93.9 ± 2.2	52.8 ± 2.3
	Tr 10	135...140	$-40.19^{+0.58}_{-0.59}$	335...375	0.5 Myr	$41.93^{+0.24}_{-0.20}$	290^{+143}_{-110}	-93.8 ± 2.2	53.1 ± 2.2
1605.3+3249	Sco-Cen	$255.09^{+0.57}_{-0.66}$	$-18.44^{+1.00}_{-1.06}$	129...171	0.5 Myr	$3.38^{+0.47}_{-0.41}$	343^{+86}_{-80}	-43.7 ± 1.6	148.8 ± 2.6
	Ext. R CrA	$261.99^{+1.12}_{-0.99}$	$-39.84^{+2.10}_{-2.00}$	70...115	0.5 Myr	$4.41^{+0.90}_{-0.85}$	321^{+109}_{-58}	-43.7 ± 1.7	148.8 ± 2.6
RBS 1223	Sco-Cen	$254.09^{+2.11}_{-2.34}$	$-6.29^{+3.23}_{-5.09}$	109^{+36}_{-19}	0.5 Myr	$4.63^{+0.84}_{-1.27}$	351^{+100}_{-104}	-210 ± 20	83 ± 18
	Ext. R CrA	$294.82^{+7.24}_{-7.92}$	$-22.94^{+4.33}_{-6.29}$	80^{+22}_{-10}	0.5 Myr	$5.78^{+1.33}_{-1.21}$	345^{+114}_{-90}	-209 ± 20	85 ± 18
	Sct OB2A	$277.15^{+2.47}_{-2.60}$	$-12.04^{+2.13}_{-1.83}$	517^{+18}_{-19}	1 Myr	$2.70^{+0.96}_{-0.44}$	75...310	-216 ± 19	53 ± 10

Table 13. Kinematic ages τ_{kin} of the four M7 members compared with their characteristic spin-down ages τ_{char} (taken from the ATNF pulsar data base (http://www.atnf.csiro.au/research/pulsar/psrcat/), Manchester et al. 2005). The fifth column gives the effective temperature as listed in table 1 of Haberl (2005) (see references therein). Column 6 gives the median masses (for TWA a mass consistent with its mass function) of the progenitor stars predicted using evolutionary models from T80, MM89 and K97 (see text) given the difference between the ages of the associations and the time since the predicted SNe.

RX J	Association	τ_{kin} (Myr)	τ_{char} (Myr)	$T_{eff,\infty}$ (10^3 K)	M_{prog} ($M_\odot$)
1856.5−3754	US	≈0.3	3.8	696	≈29
0720.4−3125	TWA	≈0.4	1.9	1044	≈10
	Tr 10	≈0.5			≈10
1605.3+3249	Sco-Cen	≈0.5	–	1113	≈29
	Ext. R CrA	≈0.5			≈15
RBS 1223	Sco-Cen	≈0.5	1.5	998	≈29
	Ext. R CrA	≈0.5			≈15
	Sct OB2	≈ 1			≈38

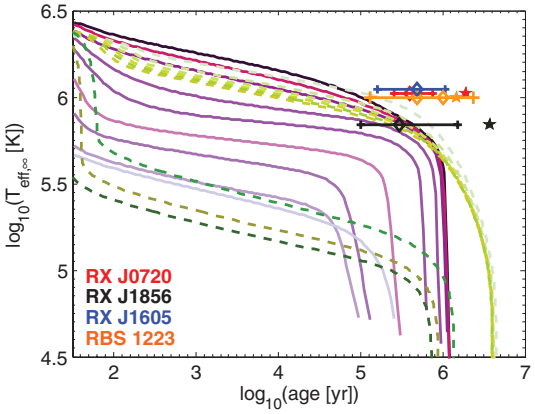

Figure 12. The four M7 members inserted into a cooling diagram. Filled stars mark the characteristic spin-down age (see Table 3) whereas horizontal lines characterize an area of the kinematic age (lower and upper values from associations in tables of Section 5). Open diamonds show the kinematic age for the associations summarized in Table 12. Effective temperatures can be found in Table 13. The purple set of cooling curves was adopted from Popov et al. (2006) (solid lines, for masses of 1.05, 1.13, 1.22, 1.28, 1.35, 1.45, 1.55, 1.65 and 1.75 $M_\odot$ from top to bottom; model from Grigorian, Blaschke & Voskresensky 2005), the green set has been kindly provided by A. D. Kaminker (dashed lines, includes superconductive protons and neutrons, for masses from 1.1 to 1.9 $M_\odot$ from top to bottom; see also Gusakov et al. 2005).

characteristic spin-down age (Table 13) that is an upper limit to the true age. From cooling models we know that, given the surface temperature, for the neutron stars investigated here, the characteristic age is too high. This is also plausible since those objects are still very young. Thus, our kinematic ages better fit with cooling models (see Fig. 12).

Since RX J1856.5-3754 is the coolest of the four M7 members investigated (RX J0720.4−3125, RX J1605.3 + 3249 and RBS 1223 show similar temperatures), it should be the oldest. However, it seems, that RX J1856.5−3754 is slightly younger than the other three (or has a similar kinematic age if we adopt the parallax of Walter et al. 2000). This might be owing to different parameters at birth or different cooling. Also the kinematic age of RX J1856.5−3754 is of about a factor of 13 smaller than its characteristic age, which is a large difference. This may indicate further doubts on the characteristic age. Mori & Ruderman (2003) propose that RX J1856.5−3754 is an isolated magnetar that has spun down by the propeller effect. In this case, dipole braking, which is assumed to calculate characteristic ages, is no longer valid. Moreover, RX J1856.5−3754 does only show a very small pulse fraction making it difficult to derive $\dot{P}$ (van Kerkwijk & Kaplan 2008).

In addition, effective temperatures may be influenced by hot spots and do not reflect the real surface temperature. Infact, this is the case for RX J0720.4−3125 (Haberl et al. 2006; Hohle et al. 2009) and RBS 1223 (Schwope et al. 2005; Haberl 2007) which appear hotter, thus must be actually shifted somewhat to smaller temperatures (even more consistent with cooling curves).

ACKNOWLEDGMENTS

We thank Thomas Eisenbeiss for data on the Her–Lyr assocation and Sergei B. Popov and Alexandr Loktin for their assistance with the preparation of our sample of OB associations and clusters. We also would like to thank Valeri V. Hambaryan for discussions and data on RBS 1223 as well as Dieter Breitschwerdt and Burkhard Fuchs for discussions on the Local Bubble. Furthermore, we thank A. D. Kaminker, Hovic Gregorian and David Blaschke for providing us their cooling curves. We also would like to thank Jos de Bruijne for discussions on the statistics and Fred Walter for carefully reading the manuscript and helping to improve the paper.

RN acknowledges general support from the German National Science Foundation (Deutsche Forschungsgemeinschaft, DFG) in grants NE 515/23-1 and SFB/TR-7, MMH and NT acknowledge partial support from DFG in the SFB/TR-7 Gravitational Wave Astronomy. The work of MMH and NT has been supported by CompStar, a research networking programme of the European Science Foundation (ESF). GM acknowledges support from the EU in the FP6 MC ToK project MTKD-CT-2006-042514. Our work has made use of the ATNF Pulsar Catalogue, version of February 2009 (Manchester et al. 2005).

We would like to thank Arnold Benz, who has motivated this study with one sentence in his new book 'Das geschenkte Universum'.

REFERENCES

Acton P. D. et al., 1993, Phys. Lett. B, 312, 501
Aharonian F. et al., 2006, A&A, 454, 775
Arzoumanian Z., Chernoff D. F., Cordes J. M., 2002, ApJ, 568, 289
Balona L. A., Laney C. D., 1995, MNRAS, 276, 627
Barrado Y Navascués D., 2006, A&A, 459, 511
Belczynski K., Taam R. E., 2008, ApJ, 685, 400
Berghöfer T. W., Breitschwerdt D., 2002, A&A, 390, 299
Bertelli G., Bressan A., Chiosi C., Fagotto F., Nasi E., 1994, A&AS, 106, 275
Beshenov G. V., Loktin A. V., 2004, Astron. Astrophys. Trans., 23, 103
Bhavya B., Mathew B., Subramaniam A., 2007, Bull. Astron. Soc. India, 35, 383
Blaauw A., 1952, Bull. Astron. Inst. Netherlands, 11, 414
Blaauw A., 1956, ApJ, 123, 408
Blaauw A., 1961, Bull. Astron. Inst. Netherlands, 15, 265
Blaauw A., 1991, in Lada C. J., Kylafis N. D., eds, NATO ASIC Proc. Vol. 342, The Physics of Star Formation and Early Stellar Evolution. Kluwer, Dordrecht, p. 125
Blaha C., Humphreys R. M., 1989, AJ, 98, 1598
Bobylev V. V., 2008, Astron. Lett., 34, 686
Brown A. G. A., Blaauw A., Hoogerwerf R., de Bruijne J. H. J., de Zeeuw P. T., 1999, in Lada C. J., Kylafis N. D., eds, NATO ASIC Proc. Vol. 540, The Origin of Stars and Planetary Systems OB Associations. Kluwer, Dordrecht, p. 411
Burrows A., Hayes J., 1996, Phys. Rev. Lett., 76, 352
Carpenter J. M., Hodapp K. W., 2008, The Monoceros R2 Molecular Cloud. p. 899
Carraro G., Chaboyer B., Perencevich J., 2006, MNRAS, 365, 867
Chatterjee S., Cordes J. M., Vlemmings W. H. T., Arzoumanian Z., Goss W. M., Lazio T. J. W., 2004, ApJ, 604, 339
Cini Castagnoli G., Bonino G., Lehman B., Taricco C., 1995, in Lucci N., Lamanna E., eds, Proc. 24th Int. Cosmic Ray Conf. Vol. 4. Int. Union of Pure and Applied Physics (IUPAP), p. 1204
Claret A., 2004, A&A, 424, 919
Clariá J. J., 1974, A&A, 37, 229
Cole A. L., Boyd R. N., Davis M. E., Thompson L. G., Davis A. M., Lewis R. S., Zinner E., 2006, ApJ, 652, 1763
Contreras M. E., Sicilia-Aguilar A., Muzerolle J., Calvet N., Berlind P., Hartmann L., 2002, AJ, 124, 1585
Cordes J. M., Chernoff D. F., 1998, ApJ, 505, 315
Dambis A. K., Mel'nik A. M., Rastorguev A. S., 2001, Astron. Lett., 27, 58
D'Antona F., Mazzitelli I., 1997, Mem. S. A. It., 68, 807
de Geus E. J., de Zeeuw P. T., Lub J., 1989, A&A, 216, 44
de la Reza R., Jilinski E., Ortega V. G., 2006, AJ, 131, 2609
de Zeeuw P. T., Hoogerwerf R., de Bruijne J. H. J., Brown A. G. A., Blaauw A., 1999, AJ, 117, 354
Dehnen W., Binney J. J., 1998, MNRAS, 298, 387
Dias W. S., Lépine J. R. D., Alessi B. S., 2002, A&A, 388, 168
Eisenbeiss T., 2007, Master's thesis, AIU, Friedrich-Schiller-Universität Jena, Germany
Ellis J., Fields B. D., Schramm D. N., 1996, ApJ, 470, 1227
Fernández D., Figueras F., Torra J., 2008, A&A, 480, 735 (F08)
Fitoussi C. et al., 2008, Phys. Rev. Lett., 101, 121101
Fuhrmann K., 2004, Astron. Nach., 325, 3
Garcia B., 1994, ApJ, 436, 705
Garmany C. D., Stencel R. E., 1992, A&AS, 94, 211
Girardi L., Bertelli G., Bressan A., Chiosi C., Groenewegen M. A. T., Marigo P., Salasnich B., Weiss A., 2002, A&A, 391, 195
Graham J. A., 1971, AJ, 76, 1079
Gregorio-Hetem J., 2008, in Reipurth B., ed., ASP Monograph Publ. Vol. 5, Handbook of Star Forming Regions Vol. II, The Southern Sky. Astron. Soc. Pac., San Francisco, p. 1
Grigorian H., Blaschke D., Voskresensky D., 2005, Phys. Rev. C, 71, 045801
Gusakov M. E., Kaminker A. D., Yakovlev D. G., Gnedin O. Y., 2005, MNRAS, 363, 555
Gvaramadze V. V., Bomans D. J., 2008, A&A, 490, 1071
Haberl F., 2005, in Briel U. G., Sembay S., Read A., eds, MPE Report 288, 5 yr of Science with XMM-Newton. MPE, Garching, p. 39
Haberl F., 2007, Ap&SS, 308, 181
Haberl F., Turolla R., de Vries C. P., Zane S., Vink J., Méndez M., Verbunt F., 2006, A&A, 451, L17
Hansen B. M. S., Phinney E. S., 1997, MNRAS, 291, 569
Harding P., Morrison H. L., Olszewski E. W., Arabadjis J., Mateo M., Dohm-Palmer R. C., Freeman K. C., Norris J. E., 2001, AJ, 122, 1397
Havlen R. J., 1972, A&A, 17, 413
Heger A., Fryer C. L., Woosley S. E., Langer N., Hartmann D. H., 2003, ApJ, 591, 288
Herbst W., Racine R., 1976, AJ, 81, 840
Herrero A., Kudritzki R. P., Vilchez J. M., Kunze D., Butler K., Haser S., 1992, A&A, 261, 209
Hobbs G., Lorimer D. R., Lyne A. G., Kramer M., 2005, MNRAS, 360, 974 (Ho05)
Hohle M. M., Haberl F., Vink J., Turolla R., Hambaryan V., Zane S., de Vries C. P., Méndez M., 2009, A&A, 498, 811
Hoogerwerf R., de Bruijne J. H. J., de Zeeuw P. T., 2001, A&A, 365, 49 (H01)
Howarth I. D., Smith K. C., 2001, MNRAS, 327, 353
Humphreys R. M., 1978, ApJS, 38, 309
Janka H.-T., Mueller E., 1996, A&A, 306, 167
Janka H.-T., Scheck L., Kifonidis K., Müller E., Plewa T., 2005, in Humphreys R., Stanek K., eds, ASP Conf. Ser. Vol. 331, The Fate of the Most Massive Stars. Astron. Soc. Pac., San Francisco, p. 363
Jilinski E., Ortega V. G., de la Reza R., 2005, ApJ, 619, 945
Johnson D. R. H., Soderblom D. R., 1987, AJ, 93, 864
Kaltcheva N., Makarov V., 2007, ApJ, 667, L155
Kaltcheva N. T., Georgiev L. N., 1994, MNRAS, 269, 289
Kaplan D., 2003, Proc. of Workshop, Physics and Astrophysics of Neutron Stars, held 2003 July 28–August 1, Santa Fe, New Mexico
Kaplan D. L., 2008, in Yuan Y.-F., Li X.-D., Lai D., eds, AIP Conf. Ser. Vol. 968, Astrophysics of Compact Objects. Am. Inst. Phys., New York, p. 129
Kaplan D. L., van Kerkwijk M. H., Anderson J., 2002, ApJ, 571, 447
Kaplan D. L., van Kerkwijk M. H., Anderson J., 2007, ApJ, 660, 1428
Kharchenko N. V., Piskunov A. E., Röser S., Schilbach E., Scholz R.-D., 2005, A&A, 440, 403
Kharchenko N. V., Scholz R.-D., Piskunov A. E., Röser S., Schilbach E., 2007, Astron. Nach., 328, 889
Kisslinger L. S., Henley E. M., Johnson M. B., 2009, Mod. Phys. Lett. A, 24, 2507
Knie K., Korschinek G., Faestermann T., Dorfi E. A., Rugel G., Wallner A., 2004, Phys. Rev. Lett., 93, 171103
Kodama T., 1997, PhD thesis, Institute of Astronomy, Univ. Tokyo (K97)
Kroupa P., Weidner C., 2005, in Corbelli E., Palla F., Zinnecker H., eds, Astrophys. Space Sci. Libr. Vol. 327, The Initial Mass Function 50 Years Later. Springer, Dordrecht, p. 175
Kuranov A. G., Popov S. B., Postnov K. A., 2009, MNRAS, 395, 2087
Lindblad B., 1959, Handb. Phys., 53, 21
Lodieu N., Bouvier J., James D. J., de Wit W. J., Palla F., McCaughrean M. J., Cuillandre J.-C., 2006, A&A, 450, 147

Loktin A. V., Beshenov G. V., 2001, Astron. Lett., 27, 386
Loktin A. V., Beshenov G. V., 2003, Astron. Rep., 47, 6
López-Santiago J., Montes D., Crespo-Chacón I., Fernández-Figueroa M. J., 2006, ApJ, 643, 1160
Lorimer D. R., Bailes M., Harrison P. A., 1997, MNRAS, 289, 592
Lozinskaia T. A., Sitnik T. G., Lomovskii A. I., 1986, Ap&SS, 121, 357
Luhman K. L., 2008, in Reipurth B., ed., ASP Monograph Vol. 5, Handbook of Star Forming Regions, Vol. II: The Southern Sky. Astron. Soc. Pac., San Francisco, p. 169
Luhman K. L., Steeghs D., 2004, ApJ, 609, 917
Lyne A. G., Lorimer D. R., 1994, Nat, 369, 127
MacConnell D. J., 1968, ApJS, 16, 275
McHargue L. R., Damon P. E., Donahue D. J., 1995, Geophys. Res. Lett., 22, 659
Madsen S., Dravins D., Lindegren L., 2002, A&A, 381, 446
Maeder A., 1987, A&A, 178, 159
Maeder A., Meynet G., 1989, A&A, 210, 155 (MM89)
Maíz-Apellániz J., 2001, ApJ, 560, L83
Maíz-Apellániz J., Walborn N. R., Galué H. A., Wei L. H., 2004, ApJS, 151, 103
Makarov V. V., 2007, ApJS, 169, 105
Manchester R. N., Hobbs G. B., Teoh A., Hobbs M., 2005, AJ, 129, 1993
Massey P., Johnson K. E., Degioia-Eastwood K., 1995, ApJ, 454, 151
Massey P., DeGioia-Eastwood K., Waterhouse E., 2001, AJ, 121, 1050
Mel'nik A. M., Efremov Y. N., 1995, Astron. Lett., 21, 10
Menten K. M., Reid M. J., Forbrich J., Brunthaler A., 2007, A&A, 474, 515
Merín B. et al., 2004, A&A, 419, 301
Mermilliod J. C., Mayor M., Udry S., 2008, A&A, 485, 303
Mermilliod J.-C., Paunzen E., 2003, A&A, 410, 511
Moffat A. F. J., Vogt N., 1973, A&AS, 10, 135
Morgan W. W., Whitford A. E., Code A. D., 1953, ApJ, 118, 318
Mori K., Ruderman M. A., 2003, ApJ, 592, L75
Motch C., Haberl F., Zickgraf F.-J., Hasinger G., Schwope A. D., 1999, A&A, 351, 177
Motch C., Zavlin V. E., Haberl F., 2003, A&A, 408, 323
Motch C., Sekiguchi K., Haberl F., Zavlin V. E., Schwope A., Pakull M. W., 2005, A&A, 429, 257
Motch C., Pires A. M., Haberl F., Schwope A., Zavlin V. E., 2007, preprint (ariXiv:0712.0342)
Motch C., Pires A. M., Haberl F., Schwope A., Zavlin V. E., 2009, A&A, 497, 423
Neuhäuser R., Guenther E. W., Petr M. G., Brandner W., Huélamo N., Alves J., 2000a, A&A, 360, L39
Neuhäuser R. et al., 2000b, A&AS, 146, 323
Ng C., Romani R. W., 2007, ApJ, 660, 1357
Penny L. R., 1996, ApJ, 463, 737
Perrot C. A., Grenier I. A., 2003, A&A, 404, 519
Perry C. L., Hill G., Christodoulou D. M., 1991, A&AS, 90, 195
Perryman M. A. C. et al., 1997, A&A, 323, L49
Pires A. M., Motch C., Turolla R., Treves A., Popov S. B., 2009, A&A, 498, 233
Popov S. B., Colpi M., Prokhorov M. E., Treves A., Turolla R., 2003, A&A, 406, 111
Popov S. B., Grigorian H., Blaschke D., 2006, Phys. Rev. C, 74, 025803
Posselt B., Popov S. B., Haberl F., Trümper J., Turolla R., Neuhäuser R., 2007, Ap&SS, 308, 171 (P07)
Preibisch T., Brown A. G. A., Bridges T., Guenther E., Zinnecker H., 2002, AJ, 124, 404
Raisbeck G. M., Yiou F., Bourles D., Lorius C., Jouzel J., 1987, Nat, 326, 273
Reichen M., Lanz T., Golay M., Huguenin D., 1990, Ap&SS, 163, 275
Reipurth B., ed., 2008a, ASP Monograph Publ. Vol. 4, Handbook of Star Forming Regions, Volume I: The Northern Sky. Astron. Soc. Pac., San Francisco
Reipurth B., ed., 2008b, ASP Monograph Publ. Vol. 5, Handbook of Star Forming Regions, Vol. II: The Southern Sky. Astron. Soc. Pac., San Francisco
Romano D., Chiappini C., Matteucci F., Tosi M., 2005, A&A, 430, 491
Rugel G. et al., 2009, Phys. Rev. Lett., 103, 072502
Rutledge R. E., Fox D. B., Shevchuk A. H., 2008, ApJ, 672, 1137
Sartori M. J., Lépine J. R. D., Dias W. S., 2003, A&A, 404, 913
Schaller G., Schaerer D., Meynet G., Maeder A., 1992, A&AS, 96, 269
Scheck L., Kifonidis K., Janka H., Müller E., 2006, A&A, 457, 963
Schild H., Maeder A., 1985, A&A, 143, L7
Schmidt-Kaler T. H., 1982, in Schaifers K., Voigt H. H., eds, Landolt-Börnstein New Ser. Vol. 2b, Physical Parameters of the Stars. Springer, New York, p. 451
Schwope A. D., Hambaryan V., Haberl F., Motch C., 2005, A&A, 441, 597
Schwope A. D., Hambaryan V., Haberl F., Motch C., 2007, Ap&SS, 308, 619
Smith N., 2006, MNRAS, 367, 763
Soderblom D. R. et al., 1998, ApJ, 498, 385
Southworth J., Maxted P. F. L., Smalley B., 2004, MNRAS, 351, 1277
Stelzer B., Neuhäuser R., 2000, A&A, 361, 581
Stone R. C., 1991, AJ, 102, 333
Terranegra L., Morale F., Spagna A., Massone G., Lattanzi M. G., 1999, A&A, 341, L79
Tetzlaff N., 2009, Master's thesis, AIU, Friedrich-Schiller-Universität Jena, Germany
Tinsley B. M., 1980, Fundamentals Cosmic Phys., 5, 287 (T80)
Torra J., Fernández D., Figueras F., 2000, A&A, 359, 82
Torres G., Mader J. A., Marschall L. A., Neuhäuser R., Duffy A. S., 2003, AJ, 125, 3237
Treves A., Popov S. B., Colpi M., Prokhorov M. E., Turolla R., 2001, in Giacconi R., Serio S., Stella L., eds, ASP Conf. Ser. Vol. 234, X-ray Astronomy 2000, The Magnificient Seven: Close-by Cooling Neutron Stars? Astron. Soc. Pac., San Francisco, p. 225
Turner D. G., 1976, ApJ, 210, 65
Turner D. G., 1979, A&A, 76, 350
Turner D. G., 1980, ApJ, 235, 146
Turner D. G., Grieve G. R., Herbst W., Harris W. E., 1980, AJ, 85, 1193
Turon C. et al., eds, 1992, The HIPPARCOS Input Catalogue, ESA Spec. Publ. Vol. 1136. ESA, Noordwijk
Uyanıker B., Fürst E., Reich W., Aschenbach B., Wielebinski R., 2001, A&A, 371, 675
van Kerkwijk M. H., Kaplan D. L., 2008, ApJ, 673, L163
van Rensbergen W., Vanbeveren D., de Loore C., 1996, A&A, 305, 825
Villamariz M. R., Herrero A., 2005, A&A, 442, 263
Walter F. M., An P., Lattimer J., Prakash M., 2000, in Martens P. C. H., Tsuruta S., Weber M. A., eds, Proc. IAU Symp. Vol. 195, Highly Energetic Physical Processes and Mechanisms for Emission from Astrophysical Plasma. Astron. Soc. Pac., San Francisco, p. 437
Walter F. M., Lattimer J. M., 2002, ApJ, 576, L145
Wang C., Lai D., Han J. L., 2006, ApJ, 639, 1007
Webb R. A., Zuckerman B., Platais I., Patience J., White R. J., Schwartz M. J., McCarthy C., 1999, ApJ, 512, L63
Westerlund B. E., 1963, MNRAS, 127, 71
Whittet D. C. B., Prusti T., Franco G. A. P., Gerakines P. A., Kilkenny D., Larson K. A., Wesselius P. R., 1997, A&A, 327, 1194
Wielen R., 1982, in Schaifers K., Voigt H. H., eds, Landolt-Börnstein New Ser. Vol. 2, Group 6, Astronomy Kinematics and Dynamics. Springer, Berlin, p. 208
Wolff S. C., Strom S. E., Dror D., Venn K., 2007, AJ, 133, 1092
Wolk S. J., Comerón F., Bourke T., 2008, in Reipurth B., ed., ASP Monograph Publ. Vol. 5, Handbook of Star Forming Regions, Vol. II: The Southern Sky. Astron. Soc. Pac., San Francisco, p. 388
Zane S., de Luca A., Mignani R. P., Turolla R., 2006, A&A, 457, 619
Zuckerman B., Song I., Bessell M. S., Webb R. A., 2001, ApJ, 562, L87
Zuckerman B., Song I., Webb R. A., 2001, ApJ, 559, 388

APPENDIX A: SAMPLE OF OB ASSOCIATIONS AND CLUSTERS

For our investigation, we selected OB associations and clusters within 3 kpc from the Sun (Table A1; for detailes on the selection criteria, please see Section 2).

Table A1. The sample of OB associations and clusters. The table gives the consecutive number, the designation, the position on the sky (J2000 galactic longitude l and latitude b), the parallax π, heliocentric velocity components U, V and W as well as estimated ages and spatial extensions either as found in the literature or obtained from angular extensions and distances. Besides Sco OB2 and YLA, U, V and W were computed as in Johnson & Soderblom (1987) (errors include proper motion and radial velocity uncertainties only). Note that ages are often uncertain to a factor of up to 2. Many OB associations contain several clusters of different ages (many of them listed here as well). The last column lists the references used for each group: A06 – Aharonian et al. (2006), B08 – Bobylev (2008), BaL95 – Balona & Laney (1995), BH89 – Blaha & Humphreys (1989) (according to Dambis et al. (2001) distances taken from this publication have been reduced by 20 per cent), Bh07 – Bhavya, Mathew & Subramaniam (2007), Bl56 – Blaauw (1956), Bl91 – Blaauw (1991), BL04 – Beshenov & Loktin (2004), Br99 – Brown et al. (1999), BYN06 – Barrado Y Navascués (2006), C06 – Carraro, Chaboyer & Perencevich (2006), CH08 – Carpenter & Hodapp (2008), Cl74 – Clariá (1974), Co02 – Contreras et al. (2002), D01 – Dambis et al. (2001), dG89 – de Geus et al. (1989), Di02 – Dias, Lépine & Alessi (2002), dlR06 – de la Reza, Jilinski & Ortega (2006), dZ99 – de Zeeuw et al. (1999), E07 – Eisenbeiss (2007), F08 – Fernández et al. (2008), Fu04 – Fuhrmann (2004), G94 – Garcia (1994), GB08 – Gvaramadze & Bomans (2008), GH08 – Gregorio-Hetem (2008), Gr71 – Graham (1971), GS92 – Garmany & Stencel (1992), H01 – Hoogerwerf et al. (2001), Ha72 – Havlen (1972), HR76 – Herbst & Racine (1976), Hu78 – Humphreys (1978), J05 – Jilinski, Ortega & de la Reza (2005), K05 – Kharchenko et al. (2005), K07 – Kharchenko et al. (2007), KG94 – Kaltcheva & Georgiev (1994), KM07 – Kaltcheva & Makarov (2007), L06 – López-Santiago et al. (2006), LB01 – Loktin & Beshenov (2001), LB03 – Loktin & Beshenov (2003), Lo06 – Lodieu et al. (2006), Loz86 – Lozinskaia, Sitnik & Lomovskii (1986), LS04 – Luhman & Steeghs (2004), Lu08 – Luhman (2008), M02 – Madsen, Dravins & Lindegren (2002), Ma07 – Makarov (2007), Mae87 – Maeder (1987), Mas95 – Massey, Johnson & Degioia-Eastwood (1995), Mas01 – Massey, DeGioia-Eastwood & Waterhouse (2001), MC68 – MacConnell (1968), ME95 – Mel'nik & Efremov (1995), Me07 – Menten et al. (2007), Mer08 – Mermilliod, Mayor & Udry (2008), Meri04 – Merín et al. (2004), MP03 – Mermilliod & Paunzen (2003WEBDA database, http://www.univie.ac.at/webda), MV73 – Moffat & Vogt (1973), Mo53 – Morgan, Whitford & Code (1953), N00 – Neuhäuser et al. (2000b), P91 – Perry, Hill & Christodoulou (1991), Pr02 – Preibisch et al. (2002), S06 – Smith (2006), Sa03 – Sartori et al. (2003), SM85 – Schild & Maeder (1985), SN00 – Stelzer & Neuhäuser (2000), So04 – Southworth, Maxted & Smalley (2004), Sod98 – Soderblom et al. (1998), T76 – Turner (1976), T79 – Turner (1979), T80a – Turner (1980), T80b – Turner et al. (1980), E07 – Eisenbeiss (2007), Te99 – Terranegra et al. (1999), U01 – Uyanıker et al. (2001), W07 – Wolff et al. (2007), We63 – Westerlund (1963), Web99 – Webb et al. (1999), Wh97 – Whittet et al. (1997), Wo08 – Wolk, Comerón & Bourke (2008), Z01a – Zuckerman et al. (2001), Z01b – Zuckerman, Song & Webb (2001).

Nr	Name	$l(^\circ)$	$b(^\circ)$	π (mas)	U(km s^{-1})	V(km s^{-1})	W(km s^{-1})	Age (Myr)	⌀(pc)	Ref.
					Scorpius OB2					
1	US	351.07	19.43	6.65	-6.7 ± 5.9	-16.0 ± 3.5	-8.0 ± 2.7	5-10	30	dG89, dZ99, Br99, M02, Pr02, Sa03, F08
2	UCL	330.51	12.86	6.96	-6.8 ± 4.6	-19.3 ± 4.7	-5.7 ± 2.5	10-20	65	dG89, dZ99, Br99, M02, Sa03, F08
3	LCC	301.54	6.74	8.38	-8.2 ± 5.1	-18.6 ± 7.3	-6.4 ± 2.6	13-20	45	dG89, dZ99, Br99, M02, Sa03, F08
					YLA					
4	TWA	291.61	20.22	16.46	-9.7 ± 4.1	-17.1 ± 3.1	-4.8 ± 3.7	8-20	66	Sod98, Web99, dlR06, BYN06, F08
5	Tuc-Hor	296.57	-51.72	23.09	-10.1 ± 2.4	-20.7 ± 2.3	-2.5 ± 3.8	10-40	100	SN00, Z01b, Ma07, F08
6	β Pic-Cap	330.95	-55.54	54.97	-10.8 ± 3.4	-15.9 ± 1.2	-9.8 ± 2.5	8-34	113	Z01a, Ma07, F08
7	ϵ Cha	300.43	-15.08	10.41	-8.6 ± 3.6	-18.6 ± 0.8	-9.3 ± 1.7	5-15	55	Te99, J05, F08
8	η Cha	292.42	-21.45	10.76	-12.2 ± 0.0	-18.1 ± 0.9	-10.1 ± 0.5	5-8	13	LS04, J05, F08
9	HD 141569	7.40	39.50	9.94	-5.4 ± 1.5	-15.6 ± 2.6	-4.4 ± 0.8	5	31	Meri04, F08
10	Ext. R CrA	359.41	-17.19	9.85	-0.1 ± 6.4	-14.8 ± 1.4	-10.1 ± 3.3	10-15	62	N00, F08
11	AB Dor	146.31	-59.00	71.43	-7.4 ± 3.2	-27.4 ± 3.2	-12.9 ± 6.4	30-120	85	L06, Ma07, F08
					Her–Lyr					
12	Her-Lyr	180.00	68.20	52.10	-13.6 ± 3.7	-22.7 ± 3.4	-7.9 ± 5.2	40-200	26	Fu04, L06, E07
					Other OB associations and clusters					
13	Sgr OB5	0.00	-1.19	0.41	-6.5 ± 10.8	1.2 ± 11.6	1.3 ± 15.0	6-12	221	SM85, BH89, D01
14	NGC 6530	6.07	-1.33	0.76	-12.1 ± 6.3	-16.2 ± 1.0	-14.3 ± 0.8	4-5	11	LB03, K05
15	Sgr OB1	7.58	-0.78	0.65	-8.0 ± 1.8	-12.8 ± 1.5	-9.5 ± 1.5	5-8	207	SM85, BH89, D01
16	Sgr OB7	10.71	-1.52	0.54	-7.4 ± 3.1	-3.2 ± 2.3	-18.6 ± 2.4	4-5	58	K05
17	Sgr OB4	12.10	-0.99	0.52	1.7 ± 3.6	-6.2 ± 7.2	-7.3 ± 12.8	<10[j]	54	Hu78, BH89, D01
18	Sgr OB6[a]	14.18	1.28	0.62	-10.8 ± 3.9	-2.8 ± 7.4	-16.0 ± 8.6	<10[j]	34	Hu78, BH89, ME95
19	M17	15.04	-0.68	0.55	-20.5 ± 12.7	9.9 ± 7.4	-21.6 ± 8.9	6	19	K05
20	Ser OB1	16.73	0.00	1.88	-4.3 ± 4.9	-3.1 ± 1.6	-2.1 ± 1.3	8-13[j]	71	Hu78, BH89, D01
21	NGC 6611	16.95	0.79	0.58	17.2 ± 0.6	5.5 ± 0.7	-5.6 ± 0.8	1-5	13	Mas95 LB03, K05, GB08
22	Sct OB3	17.32	-0.84	0.74	7.4 ± 6.1	-3.7 ± 2.6	-3.9 ± 3.8	4.5[j]	33	Hu78, BH89, D01
23	Ser OB2	18.23	1.66	0.63	-1.6 ± 1.8	-6.9 ± 2.2	-10.7 ± 0.8	4.5[j]	61	Hu78, BH89, D01
24	NGC 6604	18.25	1.71	0.59	11.9 ± 7.1	-5.2 ± 2.7	1.5 ± 1.5	4-5	15	LB03, K05
25	Sct OB2	23.21	-0.53	0.63	-8.7 ± 7.5	-7.8 ± 8.1	-4.4 ± 3.8	<6	61	SM85, BH89, D01
26	Tr 35	28.28	0.01	0.83	4.1 ± 1.9	-17.6 ± 3.3	-1.0 ± 3.6	73	2	Di02
27	Col 359	29.66	12.72	2.22	6.5 ± 0.3	-15.8 ± 0.5	-10.8 ± 0.7	28-80	17	LB03, K05, K07, Lo06, B08

Table A1 – *continued*

Nr	Name	$l(^\circ)$	$b(^\circ)$	π(mas)	U(km s^{-1})	V(km s^{-1})	W (km s^{-1})	Age (Myr)	⌀(pc)	Ref.
28	IC 4665	30.62	17.11	2.60	2.0 ± 1.5	-18.7 ± 0.9	-9.7 ± 0.6	43	13	H01, LB03, K05
29	Vul OB1	59.41	−0.12	0.63	34.4 ± 4.8	-11.3 ± 5.4	-0.8 ± 1.5	10-16[j]	230	Hu78, T80a, BH89, D01
30	NGC 6823	59.40	−0.15	0.43	63.9 ± 3.0	-18.0 ± 1.8	-0.8 ± 4.1	2-7	68	K05, W07
31	Vul OB4	60.66	−0.17	1.25	12.1 ± 2.9	-10.2 ± 3.9	-7.2 ± 2.7	10	35	T80a, BH89, D01
32	Cyg OB3	72.81	2.00	0.43	77.6 ± 2.2	-32.9 ± 2.1	-13.6 ± 3.3	8-12	106	BH89, D01, U01, So04
33	NGC 6871	72.65	2.05	0.64	49.5 ± 1.9	-25.8 ± 2.2	-10.4 ± 2.0	2-10	13	Mas95, LB03, So04, K05
34	Byurakan 1	72.75	1.75	0.63	48.9 ± 3.8	-24.0 ± 3.0	-3.4 ± 3.4	18	12	K05
35	Byurakan 2	72.75	1.34	0.58	49.8 ± 4.3	-38.4 ± 9.1	-3.3 ± 3.2	5	11	K05, Bh07
36	NGC 6883	73.28	1.18	0.48	68.8 ± 3.0	-31.3 ± 4.2	-4.6 ± 2.8	34	8	K05, A06
37	Cyg OB1	75.90	1.12	0.59	45.4 ± 2.4	-27.0 ± 1.8	-6.8 ± 2.4	7.5	142	BH89, D01, U01
38	Cyg OB8	78.02	3.30	0.81	30.1 ± 0.9	-32.4 ± 3.3	3.2 ± 2.3	3	78	BH89, D01, U01
39	Cyg OB9	78.19	1.47	1.04	26.5 ± 2.4	-22.7 ± 4.5	-6.8 ± 1.4	8	79	BH89, D01, U01
40	Cyg OB2	80.22	0.80	0.67	28.5 ± 1.7	-33.0 ± 0.3	-11.4 ± 1.8	1-5	31	Mas95, K05
41	Cyg OB4	82.80	−7.50	1.25	1.9 ± 4.5	-6.0 ± 1.0	-4.2 ± 4.1	7[j]	43	Mo53, BH89, D01
42	Cyg OB7	89.12	0.00	1.39	10.8 ± 2.4	-7.3 ± 2.3	-3.8 ± 0.7	13	163	BH89, D01, U01
43	Tr 37	99.18	3.78	1.20	19.0 ± 3.5	-12.0 ± 3.4	-6.4 ± 3.4	3-5	19	Co02, LB03, K05
44	Lac OB1	100.63	−13.22	2.72	6.6 ± 0.3	-13.3 ± 0.1	-2.7 ± 0.3	16	65	dZ99, Br99, D01
45	Cep OB2	102.09	4.42	1.63	16.1 ± 0.7	-18.2 ± 0.2	-3.1 ± 0.3	5	105	dZ99, Br99, D01
46	Cep OB1	104.19	−1.01	0.65	41.7 ± 1.6	-47.2 ± 3.0	-1.9 ± 1.5	6	322	Loz86, BH89, D01
47	Cep OB6	105.77	0.21	3.70	-14.2 ± 1.0	-24.8 ± 0.3	-5.7 ± 0.4	50	40	dZ99, Br99
48	NGC 7380	107.10	−0.88	0.45	51.3 ± 6.0	-19.9 ± 6.1	-19.8 ± 5.4	2-5	19	Mas95, LB03, K05
49	Cep OB3	110.51	2.59	1.19	15.6 ± 1.3	-17.1 ± 1.6	-7.7 ± 1.6	4[j]	29	GS92, D01, K05
50	Cas OB2	112.13	0.02	0.48	58.2 ± 6.2	-24.9 ± 12.5	-1.0 ± 4.9	10	167	Loz86, BH89, D01
51	Cas OB5	116.18	−0.33	0.50	49.6 ± 3.9	-24.1 ± 6.2	-18.6 ± 2.8	8	206	Loz86, BH89, D01
52	Cep OB4[b]	117.90	5.32	1.51	9.8 ± 3.8	-5.7 ± 4.6	-3.3 ± 4.3	2	9	MC68, BH89, GS92
53	Cas OB4	119.84	0.14	0.36	47.8 ± 7.8	-28.3 ± 9.9	-17.0 ± 5.3	8	226	Loz86, GS92, ME95, D01
54	Cas OB14	120.40	0.80	1.10	1.6 ± 4.8	-16.5 ± 4.0	5.0 ± 2.6	<10[j]	60	Hu78, BH89, D01
55	Cas OB7	122.79	1.38	0.55	34.3 ± 4.1	-21.8 ± 6.1	-8.8 ± 1.7	8	102	Loz86, GS92, ME95, D01
56	IC 1590	123.12	−6.24	0.42	34.1 ± 9.6	-24.1 ± 9.9	-11.4 ± 2.8	7	9	K05
57	Cas OB1	124.80	−1.70	0.50	39.7 ± 4.3	-24.3 ± 6.3	-13.7 ± 7.6	10	122	Loz86, BH89, D01
58	NGC 457	126.65	−4.38	0.41	42.7 ± 2.5	-9.6 ± 2.8	-23.1 ± 2.0	24	22	LB03, K05
59	Cas OB8	129.19	−1.20	0.52	30.5 ± 2.1	-17.5 ± 2.3	-8.3 ± 5.5	20[j]	43	GS92, ME95, D01
60	Per OB1	134.70	−3.10	0.43	29.2 ± 1.0	-31.1 ± 1.0	-16.0 ± 2.2	8-11	307	Mae87, ME95, D01
61	h Per	134.64	−3.72	0.48	28.8 ± 2.2	-28.3 ± 2.2	-8.6 ± 2.4	11	29	LB03, MP03, K05
62	χ Per	135.01	−3.60	0.43	30.5 ± 5.2	-24.3 ± 5.1	-9.8 ± 1.5	11	26	LB03, MP03, K05
63	Cas OB6	135.12	0.76	0.42	33.8 ± 3.8	-24.1 ± 3.8	-14.1 ± 4.5	4[j]	234	GS92, ME95, D01
64	IC 1805	134.73	0.92	0.42	40.9 ± 13.0	-25.5 ± 13.0	-30.3 ± 2.8	1-7	17	Mas95, LB03, K05
65	Cam OB1	141.24	0.91	1.13	6.7 ± 2.0	-8.7 ± 1.8	-7.2 ± 1.3	7-14	253	SM85, BH89, D01
66	NGC 1502	143.67	7.66	1.22	15.3 ± 5.2	-14.4 ± 3.9	-1.3 ± 1.5	6	6	LB03, K05
67	Cam OB3	146.95	2.88	0.29	9.1 ± 14.2	-37.4 ± 17.5	13.5 ± 8.2	11[j]	122	Hu78, ME95, D01
68	α Per	149.15	−6.36	5.65	-12.8 ± 0.3	-25.1 ± 0.6	-7.1 ± 0.2	50-71	15	dZ99, Br99, LB01, M02, BL04, K05
69	Per OB2	159.62	−16.77	3.14	-21.5 ± 0.4	-5.5 ± 1.2	-9.1 ± 0.5	4-8	41	dZ99, Br99, D01
70	Cas-Tau[c]	159.95	−12.51	5.68	-14.1 ± 5.8	-19.7 ± 3.5	-6.8 ± 1.9	50	215	Bl56, dZ99
71	Pleiades	166.63	−23.47	7.69	-6.4 ± 0.3	-26.8 ± 0.1	-13.6 ± 0.2	120	15	K05
72	Aur OB2	173.25	−0.18	0.37	1.6 ± 4.1	-0.2 ± 8.9	-11.5 ± 1.3	5.5[j]	206	Hu78, GS92, ME95, D01
73	NGC 1893	173.58	−1.68	0.30	-1.5 ± 5.2	-41.0 ± 2.2	-28.9 ± 2.2	2-3	23	Mas95, LB03, K05
74	Aur OB1	173.88	0.19	1.69	-1.0 ± 3.3	-8.4 ± 0.9	-5.6 ± 1.1	11-22[j]	120	Hu78, BH89, D01
75	NGC 2129	186.60	0.14	0.45	-8.4 ± 2.3	-37.0 ± 8.6	-7.9 ± 6.7	10	3	K05, C06
76	Gem OB1	189.00	2.30	0.49	-14.5 ± 1.5	-16.9 ± 2.9	-10.2 ± 1.9	9[j]	196	Hu78, BH89, D01
77	Mon OB1	202.07	1.07	1.74	-19.7 ± 4.6	-13.6 ± 2.6	-5.3 ± 2.2	<25	125	T76, BH89, D01
78	NGC 2264	202.95	2.20	1.52	-12.6 ± 2.1	-16.2 ± 1.0	-6.4 ± 0.5	6.5	17	LB03, K05
79	Mon OB2	206.23	−1.02	0.83	-22.1 ± 2.4	-4.5 ± 1.9	-7.2 ± 2.3	<25	179	T76, BH89, D01
80	NGC 2244	206.31	−2.08	0.69	-26.8 ± 3.1	-4.6 ± 2.0	-7.8 ± 1.6	1-5	16	Mas95, LB03, K05
81	Ori OB1	206.96	−17.53	2.43	-20.9 ± 0.8	-12.1 ± 0.5	-6.7 ± 0.5	1-11[k]	165	BH89, Bl91, Br99, D01

Table A1 – *continued*

Nr	Name	$l(^\circ)$	$b(^\circ)$	π(mas)	U(km s^{-1})	V(km s^{-1})	W(km s^{-1})	Age (Myr)	⌀(pc)	Ref.
82	λ Ori	195.27	−12.10	2.28	-27.5 ± 1.3	-14.4 ± 0.6	-8.1 ± 0.5	6	8	LB03, K05
83	NGC 1976	209.01	−19.38	2.42	-23.2 ± 2.3	-16.4 ± 1.4	-7.0 ± 1.2	51	6	K05, Me07
84	Mon R2[d]	213.91	−11.90	1.2	-11.3 ± 9.0	2.2 ± 16.6	-11.1 ± 24.4	6-10	7	HR76, CH08
85	NGC 2232	214.60	−7.41	2.74	-11.5 ± 3.7	-10.7 ± 2.6	-9.9 ± 1.2	53	8	H01, LB01, LB03, K05
86	Mon OB3[e]	217.65	−0.43	0.41	−31.6	−24.4	−0.3	7[j]	47	Gr71, BH89, ME95
87	CMa OB1	224.60	−1.50	0.61	-40.3 ± 4.2	-4.6 ± 4.1	-21.3 ± 2.3	3	102	Cl74, ME95, D01
88	IC 1848	229.07	30.40	0.50	3.6 ± 7.0	14.3 ± 7.3	-35.3 ± 6.8	4.5	24	K05
89	NGC 2287	231.02	−10.45	1.44	-16.2 ± 1.3	-13.0 ± 1.5	-18.5 ± 0.7	100-280	12	K05, GH08
90	NGC 2414	231.41	1.95	0.35	-58.9 ± 3.0	-39.4 ± 2.6	-41.8 ± 3.7	9	12	LB03, K05
91	NGC 2367	235.60	−3.84	0.50	-73.2 ± 4.5	-1.7 ± 6.0	-49.7 ± 3.3	10	12	LB03, K05
92	Col 121	237.40	−7.74	1.29	-37.4 ± 1.5	-14.9 ± 2.2	-13.9 ± 0.8	5-11	115	dZ99, Br99, D01, LB01, BL04, KM07
93	NGC 2362	238.20	−5.58	0.72	-39.9 ± 3.5	-16.2 ± 5.0	-5.3 ± 2.5	4	12	LB03, K05
94	Pup OB1[f]	243.50	0.13	0.50	-48.4 ± 17.2	-24.1 ± 16.5	5.0 ± 15.3	4	129	Ha72, Hu78, HB89, ME95
95	NGC 2467	243.16	0.35	0.74	-44.9 ± 5.4	-40.1 ± 8.8	-15.3 ± 4.7	112	9	K05
96	Col 140	245.18	−7.91	2.67	-21.2 ± 0.4	-13.8 ± 0.8	-12.1 ± 0.4	35	7	H01, LB01, K05
97	NGC 2439	245.31	−4.11	0.77	-21.6 ± 2.3	-55.7 ± 4.4	-18.8 ± 1.3	6.5	8	D01, BL04, K05
98	Col 135	248.70	−11.22	3.33	-18.3 ± 0.8	-7.0 ± 2.0	-12.7 ± 0.5	26	12	H01, LB01, LB03, K05
99	Pup OB3[b]	253.90	−0.23	0.69	-53.5 ± 15.3	-21.5 ± 12.6	-6.6 ± 14.4	4	29	We63, BH89, ME95
100	NGC 2546	254.84	−2.06	1.09	-35.4 ± 0.5	-27.5 ± 0.1	-11.0 ± 0.5	83	20	LB03, K05
101	Vel OB2	262.41	−7.52	1.97	-26.3 ± 3.1	-19.8 ± 2.7	-6.9 ± 1.3	10	70	dZ99, Br99, D01
102	Tr 10	264.38	0.47	2.73	-26.8 ± 1.8	-18.5 ± 0.2	-8.4 ± 0.7	15-35	45	dZ99, Br99, LB01, K04, BL04
103	Vel OB1	264.88	−1.42	1.13	-30.2 ± 1.3	-20.1 ± 1.7	-6.1 ± 0.8	20	120	T79, BH89, D01
104	IC 2395	266.65	−3.58	1.41	-20.6 ± 1.3	-23.6 ± 16.9	-7.0 ± 1.4	12	9	LB03, K05
105	IC 2391	270.39	−6.93	6.67	-23.5 ± 0.2	-15.6 ± 2.5	-6.3 ± 0.4	46-76	7	H01, LB01, LB03, K05
106	vdB-Hagen 99	286.62	−0.57	2.00	-27.0 ± 2.3	-14.2 ± 3.4	-15.1 ± 2.8	72	6	H01, K05
107	Car OB1	286.50	−1.49	0.53	-66.5 ± 1.0	-15.0 ± 1.6	-8.9 ± 0.9	8-12.5[j]	165	Hu78, BH89, D01
108	IC 2581	284.59	0.02	0.41	-87.5 ± 7.9	-18.0 ± 4.0	-4.5 ± 9.1	16.5	15	K05
109	NGC 3293	285.85	0.07	0.43	-90.2 ± 6.0	-12.9 ± 2.8	-12.5 ± 6.6	5-9	6	T80b, K05
110	NGC 3324	286.22	−0.18	0.43	-94.9 ± 4.2	-19.3 ± 1.2	-8.5 ± 3.7	5	13	LB03, K05
111	Tr 14	287.40	−0.58	0.36	-57.4 ± 3.3	-2.9 ± 1.1	20.0 ± 3.3	0-5	10	Mas95, LB03, K05, S06
112	Tr 15	287.41	−0.37	0.47	-57.6 ± 4.0	3.4 ± 1.6	11.5 ± 3.3	12	6	LB03, K05, Mer08
113	Tr 16	287.63	−0.65	0.35	-84.9 ± 3.6	-29.1 ± 1.6	15.2 ± 3.2	0-8	12	Mas95, LB03, K05, S06
114	Col 228	287.64	−1.06	0.52	-65.3 ± 2.7	-6.9 ± 3.2	-7.9 ± 2.5	5	23	LB03, K05
115	IC 2602	289.60	−4.90	7.14	-8.9 ± 1.1	-23.2 ± 2.8	-2.8 ± 0.5	32-67	12	H01, LB01, LB03, K05
116	Car OB2	290.41	0.09	0.39	-78.9 ± 2.4	-25.1 ± 2.3	-9.7 ± 2.4	4	152	BH89, G94, D01
117	Tr 18	290.99	−0.13	0.74	-53.2 ± 2.2	0.8 ± 0.9	-11.9 ± 2.4	59	4	LB03, K05
118	NGC 3766	294.12	−0.04	0.57	-59.8 ± 1.2	-10.9 ± 1.6	-8.3 ± 1.0	33	14	LB03, K05
119	Cru OB1	294.89	−1.08	0.61	-43.7 ± 1.6	-16.6 ± 1.9	-6.2 ± 0.8	5-7	117	BH89, KG94, D01
120	IC 2944[h]	294.85	−1.65	0.56	-46.5 ± 8.9	-14.0 ± 12.7	-24.0 ± 7.4	8	15	K05, MP03
121	Cha T	297.37	−14.25	6.15	-9.9 ± 18.9	-10.3 ± 20.2	-6.2 ± 10.8	2-6	42	Wh97, Lu08
122	Cen OB1	304.18	1.41	0.56	-45.5 ± 1.3	-6.7 ± 1.7	-8.2 ± 1.7	6-12	175	BH89, KG94, D01
123	Stock 16	306.08	0.19	0.61	-44.5 ± 5.4	19.1 ± 7.2	-2.6 ± 1.5	6	13	LB03, K05
124	Hogg 16	307.48	1.34	0.63	-52.2 ± 4.4	5.1 ± 5.4	-12.6 ± 1.4	18	5	LB03, K05
125	NGC 5606	314.84	0.99	0.55	-51.2 ± 1.9	2.6 ± 1.9	-15.3 ± 1.9	7	13	LB03, K05
126	NGC 6067	329.75	−2.21	0.71	-45.7 ± 3.6	-5.1 ± 2.2	-17.2 ± 0.8	102	12	LB03, K05
127	R 105[f]	333.10	1.90	0.62	-32.4 ± 10.5	17.0 ± 16.8	-44.5 ± 18.8	<10[j]	8	Hu78, BH89, ME95
128	Ara OB1A	337.71	−0.92	0.89	-16.0 ± 8.3	-7.8 ± 4.0	-11.6 ± 2.1	50	106	BH89, D01, Wo08
129	NGC 6193	336.71	−1.57	0.87	-38.4 ± 4.0	-7.6 ± 2.7	-13.4 ± 2.3	8	10	K05
130	NGC 6204	338.56	−1.03	0.92	-7.4 ± 1.6	-19.2 ± 4.3	1.3 ± 4.6	36	3	LB03, MP03, K05
131	Ara OB1B	337.92	−0.84	0.36	-50.0 ± 1.1	-30.7 ± 2.4	-28.8 ± 4.0	50	276	BH89, Mas95, D01, Wo08
132	Sco OB1	343.74	1.36	0.65	-29.4 ± 2.8	-2.8 ± 1.5	-5.8 ± 1.5	8	62	BH89, P91, D01
133	NGC 6231	343.46	1.19	0.80	-28.8 ± 2.9	-1.4 ± 1.0	-0.8 ± 0.7	4-7	10	BaL95, LB03, K05
134	NGC 6322	345.28	−3.05	1.00	-57.7 ± 0.2	5.5 ± 0.9	-2.7 ± 0.9	14.5	22	LB03, K05
135	Bochum 13	351.20	1.36	0.93	-5.2 ± 1.6	-17.7 ± 4.3	0.7 ± 5.1	12	4	LB03, K05
136	Sco OB4	352.40	3.44	0.91	3.9 ± 0.3	-8.5 ± 0.8	-8.5 ± 0.8	7	65	D01, K05
137	Pismis 24[i]	353.05	0.65	0.40	-3.9 ± 3.0	-13.0 ± 23.4	28.2 ± 27.0	10	4	MV73, Mas01, MP03
138	Tr 27	355.07	−0.74	0.83	-17.0 ± 0.3	-12.0 ± 3.3	-7.2 ± 3.4	30	11	LB03, K05

Table A1 – *continued*

Nr	Name	$l(^\circ)$	$b(^\circ)$	π(mas)	U(km s^{-1})	V(km s^{-1})	W(km s^{-1})	Age (Myr)	⌀(pc)	Ref.
139	NGC 6383	355.69	0.04	1.02	3.5 ± 3.2	-2.2 ± 1.7	-10.5 ± 1.8	5	9	K05
140	M6	356.62	−0.74	2.05	-12.5 ± 3.5	-16.4 ± 0.4	-3.9 ± 0.4	81	7	LB03, K05

[a] v_r from ME95, proper motion components derived from Hu78 members as median ± average deviation from median.
[b] Proper motion components and v_r derived from W63 members as median ± average deviation from median.
[c] Coordinates and parallax denote the mean of Cas-Tau members given by dZ99, velocity components reflect their median U, V, W.
[d] Proper motion components and v_r derived from CH08 members as median ± average deviation from median.
[e] Velocity components were derived from v_r only.
[f] Proper motion components and v_r derived from Hu78 members as median ± average deviation from median.
[g] Proper motion components and v_r derived from Wh97 members as median ± average deviation from median.
[h] v_r derived from WEBDA (MP03) members as median ± average deviation from median.
[i] Proper motion components and v_r derived from Mas01 members; proper motion (2 stars): mean ± maximum deviation, v_r: for only one star available (without deviation).
[j] We derived ages from HR diagrams from memberlists either from Hu78 or GS92 (Mo53 for Cyg OB4, Gr71 for Mon OB3) by fitting a set of theoretical Padova isochrones (Girardi et al. 2002) assuming solar metallicity. The fitting algorithm is based on the least-squares method and uses stellar magnitudes as weights.
[k] Ori OB1a: 11 Myr, Ori OB1b: 2 Myr, Ori OB1c: 5−11 Myr, Ori OB1d (= Trapezium cluster): ≈1 Myr.

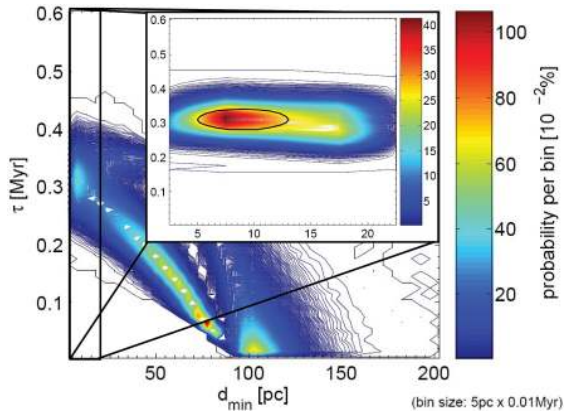

Figure B1. Distribution of the number of runs in the $\tau - d_{\rm min}$ space (excluding runs yielding $\tau = 0$) for RX J1856.5−3754 and US. The ellipse marks the region for determination of the parameters given in Table 4 and Fig. B2.

APPENDIX B: DERIVATION OF PRESENT-DAY NEUTRON STAR PARAMETERS AND SN POSITION – EXAMPLE RX J1856.5-3754 COMING FROM US

In Table 4, 6, 8 and 10, we list the current proper motions (μ^*_α, μ_δ; Columns 5 and 6), radial velocities (v_r; Column 4) and parallaxes (π; Column 8) which the neutron stars would have if they originated from the particular associations as well as the positions of the predicted SN (distance to the Sun and equatorial coordinates; Columns 9–11). Here, we describe how those values are obtained.

We first define an area within the $\tau - d_{\rm min}$ contour plot such that its boundaries reflect a 68 per cent decline from the peak (Columns 2 and 3 of the respective tables). Parameter values in Columns 4–11 were derived by selecting the input parameters (parallax, proper motion, radial velocity) which correspond to this defined region. The distance to the Sun as well as equatorial coordinates at the time of the SN were then calculated for each parameter set.

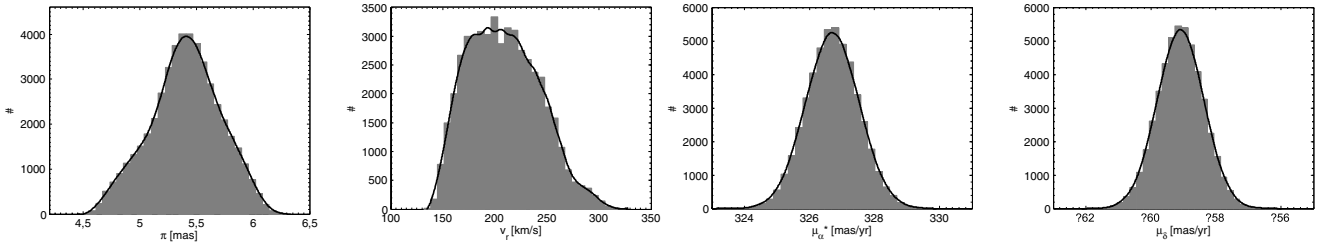

(a) Parallax π. (b) Radial velocity v_r. (c) Proper motion in right ascension μ^*_α. (d) Proper motion in declination μ_δ.

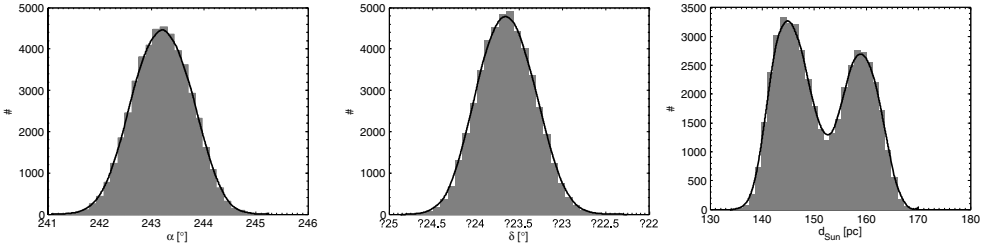

(e) Right ascension α. (f) Declination δ. (g) Distance to Sun $d_\odot$.

Figure B2. (a)–(d): distributions of present-day parameters for RX J1856.5−3754 supporting that it was created in a SN in US about 0.3 Myr ago. (e)–(g): position of the potential SN. Lines are interpolations to easier see the shape of the histogram and determine the confidence intervals of the parameters.

From the histogram of each parameter, we obtain its value and error by drawing an interpolation curve to better characterize the shape of the distribution. The 'mean' of the parameter is then given by the maximum of the curve. The error intervals include about 68 per cent of the histogram area (note that these are not 1σ errors). In the case of multiple peaks in the histogram, the interval between the two values which reflect a 68 per cent decrease of the maximum is given.

Fig. B1 gives an example of a $\tau - d_{\rm min}$ contour diagram indicating the area described above. The plot shows the distribution of minimum separations between RX J1856.5−3754 and the US centre in the $\tau - d_{\rm min}$ space. Histograms corresponding to the entries for US in Columns 4, 6 and 8–11 of Table 4 are shown in Fig. B2.

The probability of an association being the birth place of a neutron star is roughly estimated from the probability of the parallax value needed for the scenario (Gaussian distribution according to the literature value) and the probability of the necessary space velocity (adopting the distribution by Ho05). Furthermore, we are taking into account the distance of the potential SN from the centre of the association since due to a decrease of the star density with increasing distance from the centre of an association, SNe occur more likely near the centre. To account for that we make a rough estimate of the probability of a potential SN position by taking a Gaussian distribution with σ being half the radius of the association (weighted according to the number of member stars). This is justified since radii of associations are derived from star density profiles in most cases. The three probabilities are then multiplied.

This paper has been typeset from a TEX/LATEX file prepared by the author.